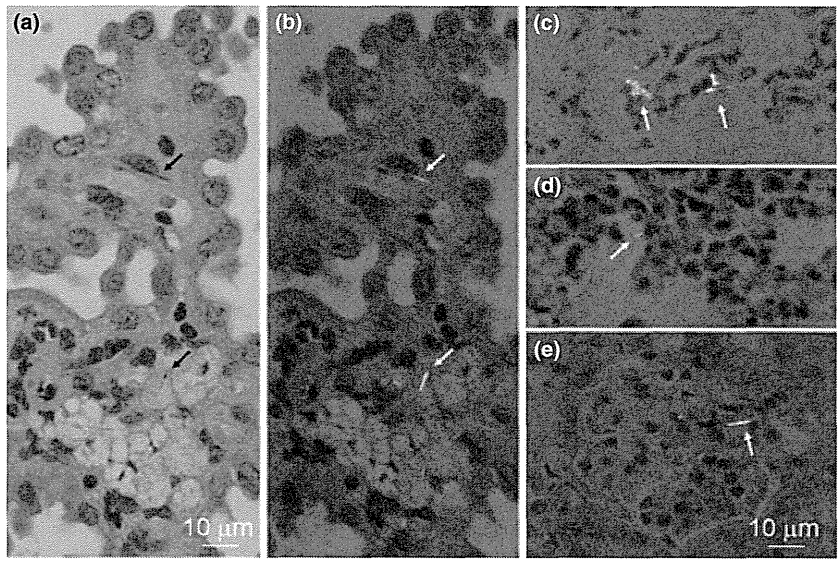

Fig. 5. Systemic distribution of singular fibers. Single micrometer-sized multi-wall carbon nanotube fibers are found in the choroid plexus in (a) normal lighting and (b) polarized light (in a mouse from the high-dose group sampled on day 168), (c) lung as an agglomerate within macrophages (polarized light) or (d) as singular fibers (polarized light) and (e) a renal glomerulus (polarized light) (in a mouse from the high-dose group sampled on day 197). Fibers were also found in hepatic sinusoids and mesenteric lymph nodes (not shown).

It is noted that the mesotheliomas of the low-dose group were not accompanied by foreign body granulomas or fibrous scars. The mesothelial atypical hyperplasia found 1 year after the i.p. injection in the low-dose group mice were also devoid of foreign body granulomas and fibrous scars. Instead, these lesions were backed up by an accumulation of mononuclear inflammatory cells. The macrophage-like cells in the accumulation, negative to weakly positive for F8/40, were often positive for singular MWCNT in their cytoplasm. As the mesothelial atypical hyperplasia is considered as precancerous lesions, the essential background of mesotheliomagenesis might be the inflammatory lesions without granulomas and fibrous scars formed against MWCNT agglomerates. The mesothelial atypical hyperplasia can be regarded as a lesion driven by the frustrated phagocytosis against MWCNT.

In general, carcinogenesis is considered a multistage process. In the case of chemical carcinogens with clear genotoxic properties, tumor onset occurs significantly earlier at higher doses.[19,20] Presumably, an increasing number of hits to a target cell leads to faster progression of the carcinogenic stages. Here, in contrast, the onset time of the mesotheliomas was apparently dose independent. Onset estimates calculated as x-intercepts of logarithmic approximation[21,22] were 126, 146, 148 and 138 days for the previous study data[2] and the three doses of the present study, respectively (Fig. S1). Mechanistically, a direct effect to a mesothelial cell, such as mutagenic or clastogenic effect, would favor a dose-dependent acceleration of the onset. If the granulomas are an important promoting factor of mesotheliomagenesis,[23] the highest dose group should have had the earliest onset because the granuloma formation can take place within 7 days subsequent to the i.p. injection.[24] In contrast, the humoral stimuli released from the nearby macrophages in the condition of frustrated phagocytosis[25] would match with this finding. As shown in Figures 3 and 4, the reactive mesothelial cells are accompanied by mononuclear inflammatory cells with MWCNT fibers, but not by epithelioid cell granulomas or fibrous scars. One could speculate that each loci of frustrated phagocytosis could continuously stimulate the nearby mesothelial cells, that is, first to induce reactive hyperplasia and then as the next step proceed towards mesothelioma. If the dose is the determinant of the number of such loci within a defined surface area of peritoneal mesothelial membrane, then it is natural to predict that the earliest day of tumor onset is dose independent, whereas the probability of tumor onset closer to the earliest day will increase in a dose-dependent manner.

An additional finding was the distribution of singular fibers to systemic organs such as the liver, mesenteric lymph nodes, pulmohilar lymph nodes, choroid plexus of the brain, glomeruli of the kidney and lung alveoli (Fig. 5). Because the brain, including the choroid plexus, lacks afferent lymphatics,[17,18] it is probable that the fibers were distributed systemically via the blood stream. Its importance to human health could be closely linked to the systemic distribution of asbestos reported in humans,[26,27] that is, a possibility of increasing systemic diseases such as cancer in various organs[28] and autoimmune diseases.[29] *In vivo* studies on the shorter fractions of MWCNT for its systemic toxicity would be essential.

It is likely that the peritoneal cavity served as a filter to segregate large agglomerates from the i.p. injected MWCNT suspension by the formation of foreign body granulomas and fibrous scars, leaving singular long MWCNT fibers for mesotheliomagenesis (frustrated phagocytosis) and short singular fibers for systemic distribution. The short fibers might have passed through the stomata (pores) of the mesothelium[23] or been transported by macrophages into lymphatics and to the vascular systems. As a whole, the i.p. injection model appears to be a robust system for the hazard identification of fiber carcinogenesis of asbestos-like fibrous particulate matter and of systemic toxicity of fibrous and non-fibrous particulate matter including nanoparticles that can enter the blood stream.

In conclusion, μm-MWCNT was mesotheliomagenic in the p53+/− mouse peritoneal cavity model in a dose-dependent manner from as low as 3 μg per mouse or approximately 10^6 fibers per mouse. Although the molecular mechanisms of fiber mesotheliomagenesis are unknown, the minute lesions seen in the lowest dose group and the dose-response characteristics might be consistent with the concept of frustrated phagocytosis and also with the observation in human asbestos epidemiology

that there would be no practical threshold for fiber mesotheliomagenesis.

Acknowledgments

The authors thank Mr Masaki Tsuji for technical support, and Dr Robert R. Maronpot and Dr Kai Savolainen for critical reading of the manuscript. The present study was supported by Health Sciences Research Grants H18-kagaku-ippan-007 and H21-kagaku-ippan-008 from the Ministry of Health, Labour and Welfare, Japan.

Disclosure Statement

The authors have no conflict of interest.

References

1 Service RF. CHEMISTRY: nanotubes: the next asbestos? *Science* 1998; **281**: 941.
2 Takagi A, Hirose A, Nishimura T *et al.* Induction of mesothelioma in p53+/− mouse by intraperitoneal application of multi-wall carbon nanotube. *J Toxicol Sci* 2008; **33**: 105–16.
3 Stanton MF, Layard M, Tegeris A *et al.* Relation of particle dimension to carcinogenicity in amphibole asbestoses and other fibrous minerals. *J Natl Cancer Inst* 1981; **67**: 965–75.
4 Pott F, Roller M, Kamino K, Bellmann B. Significance of durability of mineral fibers for their toxicity and carcinogenic potency in the abdominal cavity of rats in comparison with the low sensitivity of inhalation studies. *Environ Health Perspect* 1994; **102**(Suppl 5): 145–50.
5 Adachi S, Yoshida S, Kawamura K *et al.* Inductions of oxidative DNA damage and mesothelioma by crocidolite, with special reference to the presence of iron inside and outside of asbestos fiber. *Carcinogenesis* 1994; **15**: 753–8.
6 Roller M, Pott F, Kamino K, Althoff GH, Bellmann B. Dose-response relationship of fibrous dusts in intraperitoneal studies. *Environ Health Perspect* 1997; **105**(Suppl 5): 1253–6.
7 World Health Organization. *WHO Workshop on Mechanisms of Fibre Carcinogenesis and Assessment of Chrysotile Asbestos Substitutes*, 8–12 November 2005. Lyon, France: Summary Consensus Report World Health Organization, 2006.
8 European Chemicals Bureau. Carcinogenicity of synthetic mineral fibres after intraperitoneal injection in rats (ECB/TM/18(97) rev. 1). In: Bernstein DM, Riego Sintes JM, eds. *Methods for the Determination of the Hazardous Properties for Human Health of Man Made Mineral Fibres (MMMF) (EUR 18748 EN [1999])*. Ispra, Italy: Institute for Health and Consumer Protection, Unit: Toxicology and Chemical Substances, 1999; 41–52. [Cited 26 May 2012.] Available from URL: http://tsar.jrc.ec.europa.eu/documents/Testing-Methods/mmmfweb.pdf.
9 Marsella JM, Liu BL, Vaslet CA, Kane AB. Susceptibility of p53-deficient mice to induction of mesothelioma by crocidolite asbestos fibers. *Environ Health Perspect* 1997; **105**(Suppl 5): 1069–72.
10 Mahler JF, Flagler ND, Malarkey DE, Mann PC, Haseman JK, Eastin W. Spontaneous and chemically induced proliferative lesions in Tg.AC transgenic and p53-heterozygous mice. *Toxicol Pathol* 1998; **26**: 501–11.
11 Eastin WC, Haseman JK, Mahler JF, Bucher JR. The National Toxicology Program evaluation of genetically altered mice as predictive models for identifying carcinogens. *Toxicol Pathol* 1998; **26**: 461–73.
12 Tsukada T, Tomooka Y, Takai S *et al.* Enhanced proliferative potential in culture of cells from p53-deficient mice. *Oncogene* 1993; **8**: 3313–22.
13 Chung A, Cagle PT, Roggli VL, eds. *Tumors of the Serosal Membranes*. Washington, DC: American Registry of Pathology, 2006.
14 Chalabreysse L, Guillaud C, Tabib A, Loire R, Thivolet-Bejui F. Malignant mesothelioma with osteoblastic heterologous elements. *Ann Pathol* 2001; **21**: 428–30.
15 Matsukuma S, Aida S, Hata Y, Sugiura Y, Tamai S. Localized malignant peritoneal mesothelioma containing rhabdoid cells. *Pathol Int* 1996; **46**: 389–91.
16 Ordonez NG. Mesothelioma with rhabdoid features: an ultrastructural and immunohistochemical study of 10 cases. *Mod Pathol* 2006; **19**: 373–83.
17 Courtice FC, Simmonds WJ. The removal of protein from the subarachnoid space. *Aust J Exp Biol Med Sci* 1951; **29**: 255–63.
18 Weller RO, Djuanda E, Yow HY, Carare RO. Lymphatic drainage of the brain and the pathophysiology of neurological disease. *Acta Neuropathol* 2009; **117**: 1–14.
19 National Toxicology Program. NTP technical report on the toxicology and carcinogenesis studies of dimethyl vinyl chloride (L-chloro-2-methylpropene) (Cas No. 513-37-1) in F344/N rats and B6C3F1 mice (Gavage Studies) (NTP TR 316). National Toxicology Program, Research Triangle Park, North Carolina, 1986. [Cited 26 May 2012.] Available from URL: http://ntp.niehs.nih.gov/ntp/htdocs/lt_rpts/tr316.pdf.
20 National Toxicology Program. NTP technical report on the toxicology and carcinogenesis studies of glycidol (Cas No. 556-52-5) in F344/N rats and B6C3F1 mice (Gavage Studies) (NTP TR 374). National Toxicology Program, Research Triangle Park, North Carolina, 1990. [Cited 26 May 2012.] Available from URL: http://ntp.niehs.nih.gov/ntp/htdocs/LT_rpts/tr374.pdf.
21 Boffetta P, Burdorf A, Goldberg M, Merler E, Siemiatycki J. Towards the coordination of European research on the carcinogenic effects of asbestos. *Scand J Work Environ Health* 1998; **24**: 312–7.
22 Yano E, Wang ZM, Wang XR, Wang MZ, Lan YJ. Cancer mortality among workers exposed to amphibole-free chrysotile asbestos. *Am J Epidemiol* 2001; **154**: 538–43.
23 Donaldson K, Murphy FA, Duffin R, Poland CA. Asbestos, carbon nanotubes and the pleural mesothelium: a review of the hypothesis regarding the role of long fibre retention in the parietal pleura, inflammation and mesothelioma. *Part Fibre Toxicol* 2010; **7**: 5.
24 Poland CA, Duffin R, Kinloch I *et al.* Carbon nanotubes introduced into the abdominal cavity of mice show asbestos-like pathogenicity in a pilot study. *Nat Nanotechnol* 2008; **3**: 423–8.
25 Nagai H, Toyokuni S. Biopersistent fiber-induced inflammation and carcinogenesis: lessons learned from asbestos toward safety of fibrous nanomaterials. *Arch Biochem Biophys* 2010; **502**: 1–7.
26 Tossavainen A, Karjalainen A, Karhunen PJ. Retention of asbestos fibers in the human body. *Environ Health Perspect* 1994; **102**(Suppl 5): 253–5.
27 Miserocchi G, Sancini G, Mantegazza F, Chiappino G. Translocation pathways for inhaled asbestos fibers. *Environ Health* 2008; **7**: 4.
28 Goldsmith JR. Asbestos as a systemic carcinogen: the evidence from eleven cohorts. *Am J Ind Med* 1982; **3**: 341–8.
29 Noonan CW, Pfau JC, Larson TC, Spence MR. Nested case-control study of autoimmune disease in an asbestos-exposed population. *Environ Health Perspect* 2006; **114**: 1243–7.

Supporting Information

Additional Supporting Information may be found in the online version of this article:

Fig. S1. Estimation of the time of tumor onset.

Please note: Wiley-Blackwell are not responsible for the content or functionality of any supporting materials supplied by the authors. Any queries (other than missing material) should be directed to the corresponding author for the article.

doi: 10.1111/j.1349-7006.2012.02318.x

Cancer Science
The official journal of the Japanese Cancer Association

Multi-walled carbon nanotubes translocate into the pleural cavity and induce visceral mesothelial proliferation in rats

Jiegou Xu,[1,2] Mitsuru Futakuchi,[2] Hideo Shimizu,[3] David B. Alexander,[1] Kazuyoshi Yanagihara,[4] Katsumi Fukamachi,[2] Masumi Suzui,[2] Jun Kanno,[5] Akihiko Hirose,[6] Akio Ogata,[7] Yoshimitsu Sakamoto,[7] Dai Nakae,[7] Toyonori Omori[8] and Hiroyuki Tsuda[1,9]

[1]Laboratory of Nanotoxicology Project, Nagoya City University, Nagoya; [2]Department of Molecular Toxicology; [3]Core Laboratory, Nagoya City University Graduate School of Medical Sciences, Nagoya; [4]Department of Life Sciences, Yasuda Women's University Faculty of Pharmacy, Hiroshima; [5]Division of Cellular and Molecular Toxicology; [6]Division of Risk Assessment, National Institute of Health Sciences, Tokyo; [7]Department of Pharmaceutical and Environmental Sciences, Tokyo Metropolitan Institute of Public Health, Tokyo; [8]Department of Health Care Policy and Management, Nagoya City University Graduate School of Medical Sciences, Nagoya, Japan

(Received July 17, 2012/Revised August 20, 2012/Accepted August 22, 2012/Accepted manuscript online August 31, 2012/Article first published online October 10, 2012)

Multi-walled carbon nanotubes have a fibrous structure similar to asbestos and induce mesothelioma when injected into the peritoneal cavity. In the present study, we investigated whether carbon nanotubes administered into the lung through the trachea induce mesothelial lesions. Male F344 rats were treated with 0.5 mL of 500 μg/mL suspensions of multi-walled carbon nanotubes or crocidolite five times over a 9-day period by intrapulmonary spraying. Pleural cavity lavage fluid, lung and chest wall were then collected. Multi-walled carbon nanotubes and crocidolite were found mainly in alveolar macrophages and mediastinal lymph nodes. Importantly, the fibers were also found in the cell pellets of the pleural cavity lavage, mostly in macrophages. Both multi-walled carbon nanotube and crocidolite treatment induced hyperplastic proliferative lesions of the visceral mesothelium, with their proliferating cell nuclear antigen indices approximately 10-fold that of the vehicle control. The hyperplastic lesions were associated with inflammatory cell infiltration and inflammation-induced fibrotic lesions of the pleural tissues. The fibers were not found in the mesothelial proliferative lesions themselves. In the pleural cavity, abundant inflammatory cell infiltration, mainly composed of macrophages, was observed. Conditioned cell culture media of macrophages treated with multi-walled carbon nanotubes and crocidolite and the supernatants of pleural cavity lavage fluid from the dosed rats increased mesothelial cell proliferation *in vitro*, suggesting that mesothelial proliferative lesions were induced by inflammatory events in the lung and pleural cavity and likely mediated by macrophages. In conclusion, intrapulmonary administration of multi-walled carbon nanotubes, like asbestos, induced mesothelial proliferation potentially associated with mesothelioma development. (*Cancer Sci* 2012; 103: 2045–2050)

Multi-walled carbon nanotubes (MWCNT) are structurally composed of cylinders rolled up from several layers of graphite sheets. They are several to tens of nanometers in diameter and several to tens of micrometers in length. This high length to diameter aspect ratio, a characteristic shared with asbestos fibers, has led to concern that exposure to MWCNT might cause asbestos-like lung diseases, such as lung fibrosis, lung cancer, pleural plaque and malignant mesothelioma.[1–6]

Pleural plaque and malignant mesothelioma are characteristic lesions in asbestos-exposed humans. Although fiber dimensions, biopersistence, oxidative stress and inflammation have all been implicated,[7–12] the exact mechanisms of pleural pathogenesis are unclear. According to a pathogenesis paradigm suggested by Donaldson *et al.*,[2] asbestos fibers penetrate into the pleural cavity from the alveoli and deposit in the pleural tissue. Unlike spherical particles, fibrous materials such as asbestos are not cleared effectively from the pleural cavity, resulting in deposition of the fibers in the parietal pleura. This deposition, in turn, causes frustrated phagocytosis-induced pro-inflammatory, genotoxic and mitogenic responses in the deposition sites.[2]

Administration of MWCNT into the peritoneal cavity or scrotum in animals has been reported to induce mesothelial lesions, similar to those observed in asbestos cases.[13–15] The induction of mesothelioma in the peritonum is dose dependent, and is observed with as low as 3 μg/mouse in p53 heterozygous mice.[16] These studies suggest a potential risk that inhaled MWCNT might lead to pleural mesothelioma. However, actual experimental evidence demonstrating induction of pleural mesothelioma by inhaled MWCNT fibers has not yet been shown. It has been shown that inhaled MWCNT induced subpleural fibrosis with macrophage aggregates on the surface of the visceral pleura.[17] Notably, some of these macrophages contained MWCNT fibers. In addition, penetration of MWCNT administrated by pharyngeal aspiration into the pleural cavity was observed,[18] and intrapleural injection of 5 μg/mouse of MWCNT has been shown to lead to sustained inflammation and length-dependent retention of MWCNT in the pleural cavity.[19] Accordingly, direct interaction of MWCNT with the mesothelial tissue is postulated as an early pathogenic event.

In the present study, to examine whether MWCNT translocate into the pleural cavity and cause inflammation leading to proliferative change of the mesothelial tissue, we administered relatively high doses (five doses at 250 μg/rat) of two MWCNT samples (MWCNT-N and MWCNT-M) to the rat lung by intrapulmonary spraying (IPS)/intratracheal instillation; crocidolite (CRO; one kind of asbestos fiber) was used as a positive control. Intrapulmonary spraying has been shown to be an efficient method to deliver particle materials deep into the lung.[20–24] Our results demonstrated that MWCNT, like asbestos, translocated from the lung into the pleural cavity and induced inflammatory responses in the pleural cavity and, importantly, hyperplastic visceral mesothelial proliferation. These findings are important in understanding whether MWCNT have the potential to cause asbestos-like pleural lesions.

[9]To whom correspondence should be addressed.
E-mail: htsuda@phar.nagoya-cu.ac.jp

doi: 10.1111/cas.12005

Materials and Methods

Animals. Eight-week-old male F344 rats were purchased from Charles River Japan Inc. (Kanagawa, Japan). The animals were housed in the Animal Center of Nagoya City University Medical School and maintained on a 12 h light/12 h dark cycle, and received Oriental MF basal diet (Oriental Yeast Co. Ltd, Tokyo, Japan) and water *ad libitum*. The study was conducted according to the Guidelines for the Care and Use of Laboratory Animals of Nagoya City University Medical School and the experimental protocol was approved by the Institutional Animal Care and Use Committee (H22M-19).

Preparation of MWCNT and CRO suspensions. The MWCNT investigated were MWCNT-N (Nikkiso Co., Ltd, Tokyo, Japan) and MWCNT-7 (Mitsui Chemicals Inc., Tokyo, Japan; designated as MWCNT-M). Crocidolite (Union for International Cancer Control grade) was from the National Institute of Health Sciences of Japan stocks. Ten milligrams of MWCNT-N or MWCNT-M were suspended in 20 mL of saline containing 0.1% Tween 20 and homogenized for 1 min four times at 3000 r.p.m. in a Polytron PT1600E benchtop homogenizer (Kinematika AG, Littau, Switzerland). The suspensions were sonicated for 30 min shortly before use to minimize aggregation. The CRO suspension was prepared similarly, but without homogenization. The concentration of the MWCNT and CRO suspensions was 500 μg/mL. The lengths of MWCNT and CRO in the suspensions were determined using a digital map meter (Comcureve-9 Junior; Koizumi Sokki MFG. Co., Ltd, Nigata, Japan) on scanning electron microscope (SEM) photos. The SEM observation and length distributions of MWCNT and CRO are shown in Fig. S1A,B. To count the fiber number, 500 μg/mL suspensions of MWCNT-N, MWCNT-M and CRO were diluted 1:1000 with deionized water and 0.5 μL of the diluted suspensions was loaded onto clean glass slides and dried in a micro oven at 480°C for 1 min. The fiber number on the slides was counted under a polarized light microscope (PLM) (Olympus BX51N-31P-O PLM, Tokyo, Japan) (PLM detects all fibers longer than 200 nm). The results are shown in Fig. S1C.

Intrapulmonary spraying of MWCNT and CRO into the lung and pleural cavity lavage (PCL). We used the intrapulmonary spraying technique that was developed in our laboratory.[24] Briefly, rats were anaesthetized using isoflurane; the mouth was fully opened with the tongue gently held and the nozzle of a microsprayer (series IA-1B Intratracheal Aerosolizer; Penn-century, Philadelphia, PA, USA) was inserted into the trachea through the larynx and 0.5 mL suspension was sprayed into the lungs synchronizing with spontaneous respiratory inhalation. We confirmed that the dosed materials were distributed deep into the lung tissue and reached most of the terminal alveoli without causing obvious respiratory distress.

Ten-week-old male Fisher 344 rats were divided into four groups of six animals each and given 0.5 mL of saline containing 0.1% Tween 20 or 500 μg/mL MWCNT-N, MWCNT-M or CRO suspension by IPS once every other day five times over a 9-day period. The total amount of fibers administered was 1.25 mg/rat. Six hours after the last IPS, the rats were placed under deep isoflurane anesthesia; a small incision was made in the abdominal wall, the pleural cavity was injected with 10 mL of ice cold RPMI 1640 through the diaphragm, and the lavage fluid was collected by syringe. The rats were then killed by exsanguination from the inferior vena cava and the major organs, including the lung, chest wall, brain, liver, kidney, spleen and mediastinal lymph nodes, were fixed in 4% paraformaldehyde and processed for histological examination.

Analysis of inflammatory reaction in the pleural cavity. Cells in the lavage fluid were counted using a hemocytometer (Erma Co., Ltd, Tokyo, Japan), and the cellular fraction was then isolated by centrifugation at 200*g* for 5 min at 4°C. Cell pellets collected from three rats were combined (generating a total of two cell pellets per group), fixed in 4% paraformaldehyde and processed for histological examination. Total protein in the supernatants of each of the lavage fluids was determined using the Pierce BCA Protein Assay Kit (Thermo Scientific, Rockford, IL, USA) and the supernatants were then concentrated by centrifugation in Vivaspin 15 concentrators (Sartorius Stedium Biotech, Goettingen, Germany) at 1500*g* for 30 min at 4°C and used for *in vitro* cell proliferation assays.

Light microscopy and PLM. Haematoxylin–eosin (H&E)-stained slides of the lung tissues and cellular pellets of the PCL were used to observe MWCNT-N, MWCNT-M and CRO fibers with PLM at ×1000 magnification. The exact localization of the illuminated fibers was confirmed in the same H&E-stained sections after removing the polarizing filter.

Scanning electron microscopy. The H&E-stained slides of the lung tissue and PCL pellets were immersed in xylene for 3 days to remove the cover glass, then immersed in 100% ethanol for 10 min to remove the xylene and air-dried for 2 h at room temperature. The slides were then coated with platinum for viewing using a scanning electronic microscope (SEM) (Model S-4700 Field Emission SEM; Hitachi High Technologies Corporation, Tokyo, Japan) at 5–10 kV.

Immunohistochemistry and Azan–Mallory staining. CD68, proliferating cell nuclear antigen (PCNA) and mesothelin/Erc were detected using antirat CD68 antibodies (BMA Biomedicals, Augst, Switzerland), anti-PCNA monoclonal antibodies (Clone PC10; Dako Japan Inc., Tokyo, Japan) and antirat C-ERC/mesothelin polyclonal antibodies (Immuno-Biological Laboratories Co., Ltd, Gunma, Japan). The CD68, PCNA and C-ERC/mesothelin antibodies were diluted 1:100, 1:200 and 1:1000, respectively, in blocking solution and applied to deparaffinized slides. The slides were incubated at 4°C overnight and then incubated for 1 h with biotinylated species-specific secondary antibodies diluted 1:500 (Vector Laboratories, Burlingame, CA, USA) and visualized using avidin-conjugated horseradish peroxidase complex (ABC kit; Vector Laboratories). Azan–Mallory staining was used to visualize collagen fibers.

***In vitro* exposure and preparation of conditioned macrophage culture media.** The induction and preparation of primary alveolar macrophages (PAM) has been described previously.[24] PAM were seeded into 6 cm culture dishes at 2×10^6 cells per well in 10% FBS RPMI 1640. After overnight incubation, the culture media was refreshed and MWCNT-N, MWCNT-M or CRO suspensions were added to the cells to a final concentration of 10 μg/mL. The cells were then incubated for another 24 h. The conditioned macrophage culture media was then collected for *in vitro* cell proliferation assays.

***In vitro* cell proliferation assay.** Human mesothelioma cells, TCC-MESO1, derived from a patient in the Tochigi Cancer Center,[25] were seeded into 96-well culture plates at 2×10^3 cells per well in 10% FBS RPMI 1640. After overnight incubation, the cells were serum-starved for 24 h. The media was changed to 100 μL of the concentrated supernatants of the PCL or conditioned macrophage culture media and incubated for 72 h. The relative cell number was then determined using the Cell Counting Kit-8 (Dojindo Molecular Technologies, Rockville, MD, USA) according to the manufacturer's instruction.

Statistical analysis. Statistical analysis was performed using ANOVA. The statistical significance was analyzed using a two-tailed Student's *t*-test. A *P*-value of <0.05 was considered to be significant.

Results

Translocation of MWCNT and CRO fibers into the pleural cavity. The cell pellets of the PCL were used to examine whether

doi: 10.1111/cas.12005

the MWCNT or CRO fibers were present in the pleural cavity. We first screened the H&E-stained PCL cell pellet slides using PLM. The exact localization of the fibers was confirmed using SEM of the same slide sections. MWCNT-N, MWCNT-M and CRO fibers were present in PCL cell pellets, with most of the fibers in macrophage-like cells (Fig. 1a–c) with very few fibers located in the intercellular space or on cell surfaces (data not shown). Immunohistochemistry with CD68, a macrophage marker, showed that MWCNT and CRO fibers were mainly found in macrophages (Fig. 1d,e).

In tissue sections, MWCNT and CRO fibers were mainly detected in focal granulomatous lesions in the alveoli and in alveolar macrophages. Fibers were also found in the mediastinal lymph nodes, and a few fibers were detected in liver sinusoid cells, blood vessel wall cells in the brain, renal tubular cells and spleen sinus and macrophages (data not shown). We detected only a few fibers penetrating directly from the lung to the pleural cavity through the visceral pleura (Fig. S2) and did not find any fibers in the parietal pleura.

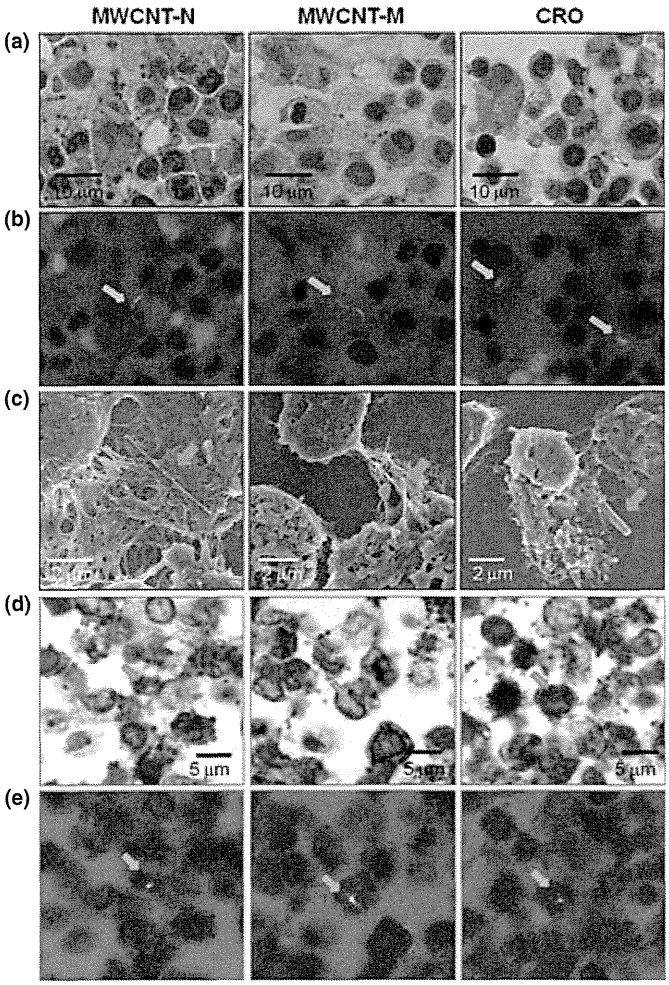

Fig. 1. Existence of multi-walled carbon nanotubes (MWCNT)-N, MWCNT-M and crocidolite (CRO) fibers in the cell pellets of the pleural cavity lavage (PCL). (a) Images of H&E-stained slides of the cell pellets of the PCL treated with MWCNT-N, MWCNT-M and CRO fibers. (b) Polarized light microscope (PLM) images of the same view areas shown in (a). (c) Scanning electron microscope observation showed the existence of the MWCNT and CRO fibers in the cell pellets of the PCL. (d) CD68 immunostaining of the PCL cell pellet slides. (e) PLM observation of the same view areas shown in (d) indicate that MWCNT and CRO fibers were present in the CD68-positive macrophages. Arrows indicate MWCNT-N, MWCNT-M and CRO fibers.

Induction of visceral mesothelial proliferation. Hyperplastic visceral mesothelial proliferation (HVMP) was clearly observed in all of the MWCNT and CRO treated groups. The HVMP lesions were composed of mesothelial cells with cuboidal appearance and increased size and density lining the visceral pleural tissue. Various degrees of lung inflammation and fibrous thickening were observed underneath the HVMP lesions (Fig. 2a, panel A). The PCNA immunostaining showed proliferating mesothelial cells within the HVMP lesions (Fig. 2a, panel B). The PCNA indices of the visceral mesothelium were increased approximately 10-fold in all the MWCNT and CRO treated groups compared with the control group

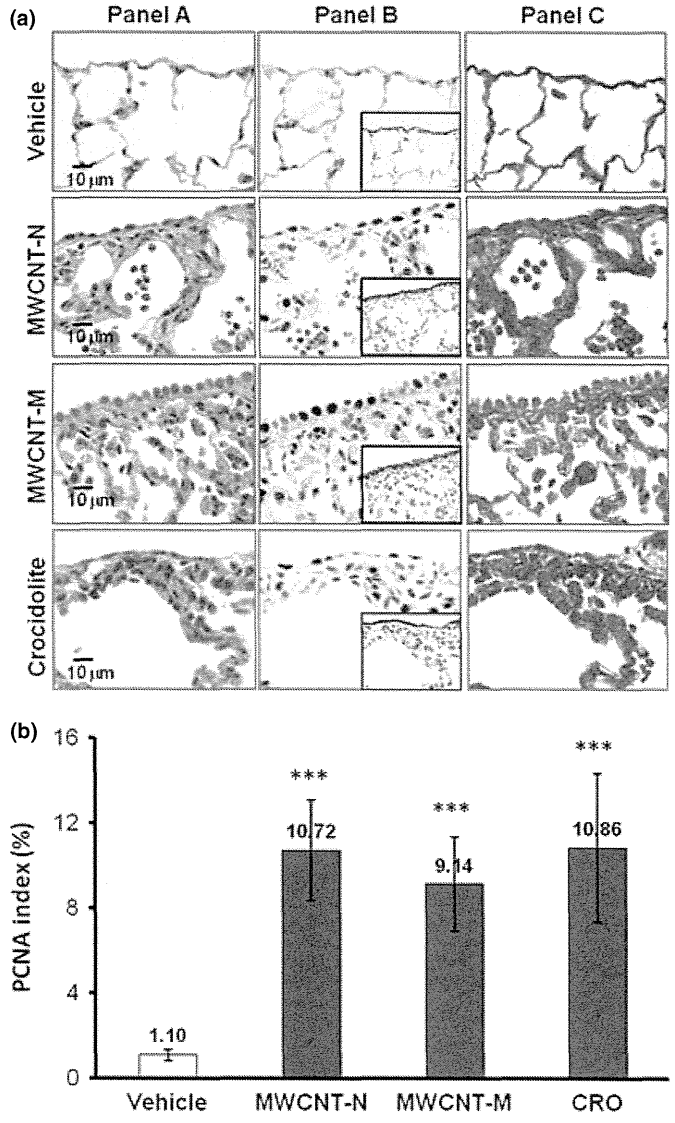

Fig. 2. Induction of visceral mesothelial cell proliferation lesions by treatment with multi-walled carbon nanotubes (MWCNT)-N, MWCNT-M or crocidolite (CRO). (a) Serial sections were prepared and stained with H&E, proliferating cell nuclear antigen (PCNA), Erc/mesothelin and Azan–Mallory's collagen staining. Panel A: increase in enlarged visceral mesothelial cells with cuboidal shapes in the MWCNT-N, MWCNT-M and CRO treated groups. Panel B: PCNA-positive cells are clearly increased in the dosed groups. The inserts are immunostained with Erc/mesothelin and show the lining of the mesothelium. Panel C: Azan–Mallory's staining; sub-pleural collagenous fibrosis is present under the mesothelial cell proliferation lesions. (b) PCNA index, expressed as the percentage of PCNA-positive cells of the total number of visceral mesothelial cells per slide. ***$P < 0.001$.

(Fig. 2b). Azan–Mallory staining showed increases in collagen fibers underneath the HVMP lesions (Fig. 2a, panel C). Fibers were not found within the HVMP lesions themselves. Alveolar macrophages with phagocytosed MWCNT or CRO fibers were frequently observed near the HVMP lesions (Fig. S3). Proliferation and other lesions of the parietal mesothelium were not observed.

Inflammatory cell infiltration in the pleural cavity. Both MWCNT and CRO treatment resulted in inflammatory reactions in the pleural cavity. The total number of cells, composed mostly of macrophages, neutrophils and lymphocytes, in the PCL in the MWCNT and CRO treated groups was significantly increased compared with the control group (Fig. 3a). As can be calculated from Fig. 3(a,b), macrophages accounted for a large part of the increase of the total cell number in the PCL, although the number of neutrophils and lymphocytes also increased. Overall, the proportion of macrophages in the cell pellets of the PCL was increased, while those of neutrophils and lymphocytes were decreased (Fig. 3b). MWCNT or CRO treatment also significantly increased the total protein level in the PLC (Fig. 3c). The proportion of cells in the PCL pellets positive for Mesothelin/Erc, a mesothelial cell marker, was 0.53–1.02%, and no intergroup difference was observed (data not shown). These data indicate that the increased cell number in the pleural cavity of the rats treated with MWCNT or CRO resulted from inflammatory cell effusion, not from mesothelial cell shedding of the pleural tissue. Many macrophages in the PCL contained MWCNT or CRO fibers.

Mesothelial cell proliferation assay *in vitro*. To examine whether inflammatory reactions, especially those mediated by macrophages, exert proliferative effects on mesothelial cells, we examined the effects of conditioned macrophage culture medium on mesothelial cell proliferation *in vitro*. The conditioned culture media of macrophages exposed to MWCNT-N, MWCNT-M or CRO significantly increased the proliferation of the human mesothelioma cell line TCC-MESO1. The concentrated supernatants of the PCL taken from the rats treated with MWCNT-N, MWCNT-M or CRO exhibited similar effects (Fig. 4). These results indicate that factors in the PCL, possibly secreted by alveolar and pleural macrophages, are able to cause mesothelial cell proliferation.

Discussion

In the present study, we compared the pleural translocation of MWCNT and CRO and examined the mesothelial lesions they induced. Our data demonstrate that after deposition in the lung, MWCNT, like CRO, translocated into the pleural cavity, mainly in pleural macrophages. Both MWCNT and CRO treatment also caused hyperplastic visceral mesothelial proliferation and marked pleural inflammation.

This is the first report to show that MWCNT administered into the rat lung causes mesothelial proliferative lesions. Adamson *et al.*[26] reported that intratracheal instillation of asbestos in mice induced pleural mesothelial cell proliferation within several days; the degree of pleural mesothelial cell proliferation did not appear to correlate with the localization of asbestos fibers in the pleura.[27] Similarly, we did not find fibers within the HVMP lesions. Thus, our findings suggest that HVMP lesions do not appear to be directly induced by the deposited MWCNT or CRO fibers. Also, *in vitro* exposure to MWCNT and CRO fibers did not lead to proliferation of TCC-MESO1 cells, but rather to cell death (Fig. S4). It has been reported that macrophages play a significant role in mesothelial cell proliferation caused by asbestos exposure and surgical injury,[28–31] and that the conditioned medium of macrophages

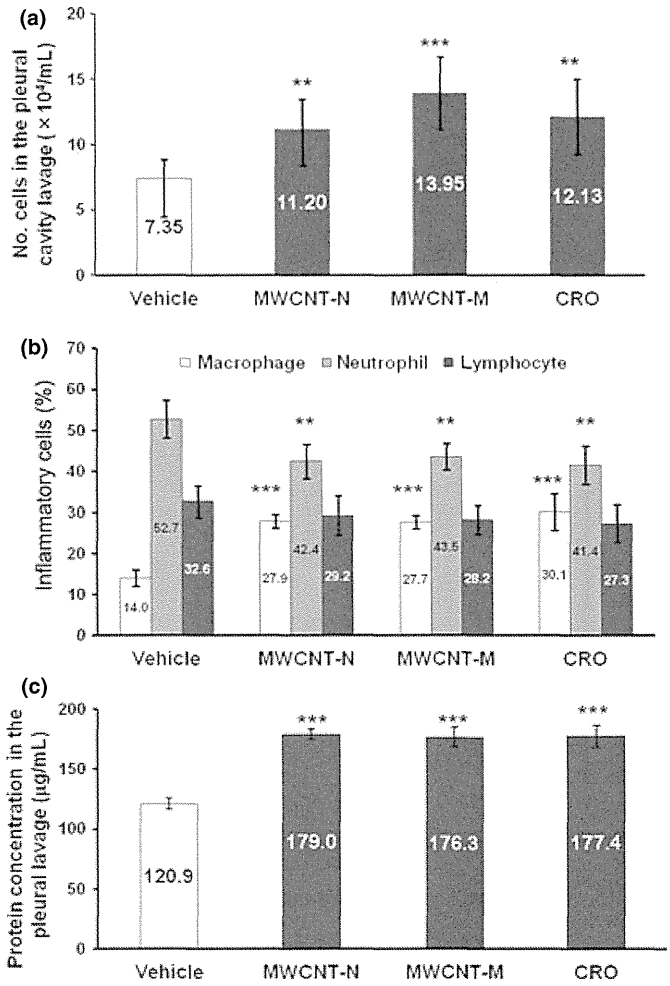

Fig. 3. Inflammatory reaction in the pleural cavity. (a) The number of leukocytes in the pleural cavity lavage (PCL) of rats treated with multi-walled carbon nanotubes (MWCNT) and crocidolite (CRO). (b) The proportion of macrophages, neutrophils and lymphocytes in the cell pellets of the PCL. Total cell number and cell numbers of macrophages, neutrophils and lymphocytes in 10 randomly chosen fields (×400) were counted. (c) Protein concentration in the supernatants of the PCL. $^{**}P < 0.01$; $^{***}P < 0.001$.

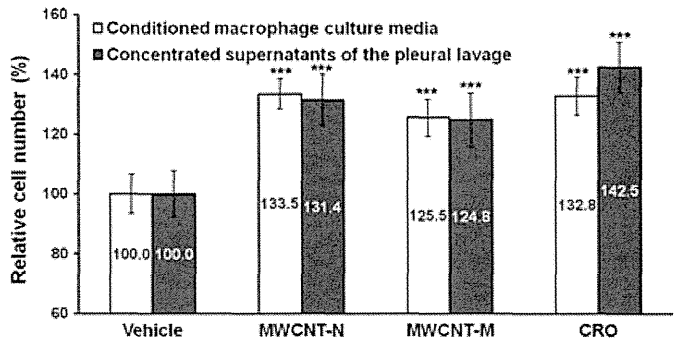

Fig. 4. Effect of conditioned macrophage culture media and the supernatants of the pleural cavity lavage (PCL) on mesothelial cell proliferation *in vitro*. The conditioned culture media of macrophages treated with multi-walled carbon nanotubes (MWCNT)-N, MWCNT-M or crocidolite (CRO) significantly increased the cell proliferation of TCC-MESO1. The concentrated supernatants of the PCL from the rats treated with MWCNT-N, MWCNT-M or CRO had similar effects. $n = 6$. $^{***}P < 0.001$.

doi: 10.1111/cas.12005

exposed to MWCNT promotes mesothelial cell proliferation *in vitro*.[30] Activated macrophages secrete a panel of growth factors and cytokines to regulate cell proliferation, which can augment transformation of mesothelial cells.[28,30,32,33] Our observations that mesothelial cell proliferation is enhanced by conditioned macrophage culture media and by the supernatants of pleural cavity lavage are consistent with these results, although the factors that are involved need to be identified.

Translocation of asbestos[34,35] and MWCNT[18] fibers from the lung to the pleural cavity has been found in rodents. This translocation also probably occurs in humans since asbestos fibers have been detected in human pleural lesions.[36] However, the mechanism and route of translocation are unclear. It has been suggested that penetration through the visceral pleura, possibly driven by increased pulmonary interstitial pressure and assisted by enhanced permeability of the visceral pleura due to asbestos-induced inflammation might be a major route.[37] In the present study, only a few MWCNT and CRO fibers were observed penetrating through the visceral pleura, and a large number of the fibers in the pleural cavity was observed in macrophages. We also observed frequent deposition of MWCNT and CRO in the mediastinal lymph nodes, mostly phagocytosed by macrophages. These results suggest that a probable route of translocation of the fibers is lymphatic flow. Inflammation in the pleural cavity is probably a defense response against translocated fibers. Murphy *et al.*[19] reported that intrapleural injection of 5 μg/mouse of long MWCNT or asbestos initiated sustained inflammation, including increased granulocyte number and protein level, in the pleural cavity. Thus, the observed proliferation of visceral mesothelial cells in the present study is probably caused by inflammatory reactions both in the lung and in the pleural cavity. In the present study, no MWCNT or crosidolite fibers or lesions were observed in the parietal pleura. This is possibly due to the short experimental period and limited amount of fibers in the pleural cavity, which would result in little inflammation in the parietal pleura.

Currently, the exposure level to MWCNT in the workplace is unknown and there are no administrational regulations for the occupational exposure limit for MWCNT. In November 2010, the National Institute of Occupational Safety and Health (NIOSH) released a non-official carbon nanotube exposure limit for peer review. The recommended exposure limit in the air was set at 7 $\mu g/m^3$.[38] Previously, we used a total dose of 1.25 mg/rat of titanium dioxide over a 9-day period and identified factors involved in titanium dioxide-induced lung lesions.[24] In the present study, we used the same protocol for the purpose of induction of observable pleural lesions and inflammation in the pleural cavity as well to ensure the presence of a detectable number of fibers in the pleural cavity after short-term administration; this dose was higher than the NIOSH exposure limit. Time- and dose-dependent experiments are needed in future studies, and further investigation is also required to elucidate cytokines and other factors that cause parietal mesothelial proliferation in animal models that are more relevant to humans.

The IPS/intratracheal instillation is a widely used method to evaluate the respiratory toxicity of particles. It should be noted that IPS/intratracheal instillation is a non-physiological method and possibly affects the migration and distribution of particles in the lung due to the pressure from spraying. However, IPS/intratracheal instillation is relevant for identifying factors to be examined using long-term, more physiologically relevant methods of CNT administration.

In summary, MWCNT and CRO fibers were found to translocate from the lung to the pleural cavity after intrapulmonary administration. Importantly, MWCNT and CRO treatment caused visceral mesothelial cell proliferation and inflammation in the pleural cavity. This mesothelial proliferation was plausibly induced by inflammatory events in the lung and pleural cavity and mediated primarily by macrophages. The similarity between MWCNT-N, MWCNT-M and CRO in translocation to the pleural cavity, induction of pleural cavity inflammation and induction of visceral pleural mesothelial proliferation suggests that MWCNT might cause asbestos-like pleural lesions.

Acknowledgments

This work was supported by Health and Labour Sciences Research Grants (Research on Risk of Chemical Substance 21340601) (grant numbers H19-kagaku-ippan-006, H22-kagaku-ippan-005).

Disclosure Statement

The authors have no conflict of interest.

References

1 Bonner JC. Nanoparticles as a potential cause of pleural and interstitial lung disease. *Proc Am Thorac Soc* 2010; **7**: 138–41.
2 Donaldson K, Murphy FA, Duffin R *et al.* Asbestos, carbon nanotubes and the pleural mesothelium: a review of the hypothesis regarding the role of long fibre retention in the parietal pleura, inflammation and mesothelioma. *Part Fibre Toxicol* 2010; **7**: 5.
3 Johnston HJ, Hutchison GR, Christensen FM *et al.* A critical review of the biological mechanisms underlying the *in vivo* and *in vitro* toxicity of carbon nanotubes: the contribution of physico-chemical characteristics. *Nanotoxicology* 2010; **4**: 207–46.
4 Nagai H, Toyokuni S. Biopersistent fiber-induced inflammation and carcinogenesis: lessons learned from asbestos toward safety of fibrous nanomaterials. *Arch Biochem Biophys* 2010; **502**: 1–7.
5 Pacurari M, Castranova V, Vallyathan V. Single- and multi-wall carbon nanotubes versus asbestos: are the carbon nanotubes a new health risk to humans? *J Toxicol Environ Health A* 2010; **73**: 378–95.
6 Tsuda H, Xu J, Sakai Y *et al.* Toxicology of engineered nanomaterials – a review of carcinogenic potential. *Asian Pac J Cancer Prev* 2009; **10**: 975–80.
7 Barrett JC. Cellular and molecular mechanisms of asbestos carcinogenicity: implications for biopersistence. *Environ Health Perspect* 1994; **102** (Suppl 5): 19–23.
8 Miller BG, Searl A, Davis JM *et al.* Influence of fibre length, dissolution and biopersistence on the production of mesothelioma in the rat peritoneal cavity. *Ann Occup Hyg* 1999; **43**: 155–66.
9 Okada F. Beyond foreign-body-induced carcinogenesis: impact of reactive oxygen species derived from inflammatory cells in tumorigenic conversion and tumor progression. *Int J Cancer* 2007; **121**: 2364–72.
10 Stanton MF, Wrench C. Mechanisms of mesothelioma induction with asbestos and fibrous glass. *J Natl Cancer Inst* 1972; **48**: 797–821.
11 Walker C, Everitt J, Barrett JC. Possible cellular and molecular mechanisms for asbestos carcinogenicity. *Am J Ind Med* 1992; **21**: 253–73.
12 Yang H, Testa JR, Carbone M. Mesothelioma epidemiology, carcinogenesis, and pathogenesis. *Curr Treat Options Oncol* 2008; **9**: 147–57.
13 Poland CA, Duffin R, Kinloch I *et al.* Carbon nanotubes introduced into the abdominal cavity of mice show asbestos-like pathogenicity in a pilot study. *Nat Nanotechnol* 2008; **3**: 423–8.
14 Sakamoto Y, Nakae D, Fukumori N *et al.* Induction of mesothelioma by a single intrascrotal administration of multi-wall carbon nanotube in intact male Fischer 344 rats. *J Toxicol Sci* 2009; **34**: 65–76.
15 Takagi A, Hirose A, Nishimura T *et al.* Induction of mesothelioma in p53+/− mouse by intraperitoneal application of multi-wall carbon nanotube. *J Toxicol Sci* 2008; **33**: 105–16.
16 Takagi A, Hirose A, Futakuchi M *et al.* Dose-dependent mesothelioma induction by intraperitoneal administration of multi-wall carbon nanotubes in p53 heterozygous mice. *Cancer Sci* 2012; **103**: 1440–4.
17 Ryman-Rasmussen JP, Cesta MF, Brody AR *et al.* Inhaled carbon nanotubes reach the subpleural tissue in mice. *Nat Nanotechnol* 2009; **4**: 747–51.
18 Mercer RR, Hubbs AF, Scabilloni JF *et al.* Distribution and persistence of pleural penetrations by multi-walled carbon nanotubes. *Part Fibre Toxicol* 2010; **7**: 28.

19 Murphy FA, Poland CA, Duffin R *et al.* Length-dependent retention of carbon nanotubes in the pleural space of mice initiates sustained inflammation and progressive fibrosis on the parietal pleura. *Am J Pathol* 2011; **178**: 2587–600.
20 Oka Y, Mitsui M, Kitahashi T *et al.* A reliable method for intratracheal instillation of materials to the entire lung in rats. *J Toxicol Pathol* 2006; **19**: 107–9.
21 Jackson P, Hougaard KS, Boisen AM *et al.* Pulmonary exposure to carbon black by inhalation or instillation in pregnant mice: effects on liver DNA strand breaks in dams and offspring. *Nanotoxicology* 2012; **6**: 486–500.
22 Morimoto Y, Hirohashi M, Ogami A *et al.* Pulmonary toxicity of well-dispersed multi-wall carbon nanotubes following inhalation and intratracheal instillation. *Nanotoxicology* 2012; **6**: 587–99.
23 Ogami A, Yamamoto K, Morimoto Y *et al.* Pathological features of rat lung following inhalation and intratracheal instillation of C(60) fullerene. *Inhal Toxicol* 2011; **23**: 407–16.
24 Xu J, Futakuchi M, Iigo M *et al.* Involvement of macrophage inflammatory protein 1alpha (MIP1alpha) in promotion of rat lung and mammary carcinogenic activity of nanoscale titanium dioxide particles administered by intrapulmonary spraying. *Carcinogenesis* 2010; **31**: 927–35.
25 Yanagihara K, Tsumuraya M, Takigahira M *et al.* An orthotopic implantation mouse model of human malignant pleural mesothelioma for *in vivo* photon counting analysis and evaluation of the effect of S-1 therapy. *Int J Cancer* 2010; **126**: 2835–46.
26 Adamson IY, Bakowska J, Bowden DH. Mesothelial cell proliferation after instillation of long or short asbestos fibers into mouse lung. *Am J Pathol* 1993; **142**: 1209–16.
27 Sekhon H, Wright J, Churg A. Effects of cigarette smoke and asbestos on airway, vascular and mesothelial cell proliferation. *Int J Exp Pathol* 1995; **76**: 411–8.
28 Adamson IY, Prieditis H, Young L. Lung mesothelial cell and fibroblast responses to pleural and alveolar macrophage supernatants and to lavage fluids from crocidolite-exposed rats. *Am J Respir Cell Mol Biol* 1997; **16**: 650–6.
29 Li XY, Lamb D, Donaldson K. Mesothelial cell injury caused by pleural leukocytes from rats treated with intratracheal instillation of crocidolite asbestos or *Corynebacterium parvum*. *Environ Res* 1994; **64**: 181–91.
30 Murphy FA, Schinwald A, Poland CA *et al.* The mechanism of pleural inflammation by long carbon nanotubes: interaction of long fibres with macrophages stimulates them to amplify pro-inflammatory responses in mesothelial cells. *Part Fibre Toxicol* 2012; **9**: 8.
31 Mutsaers SE, Whitaker D, Papadimitriou JM. Stimulation of mesothelial cell proliferation by exudate macrophages enhances serosal wound healing in a murine model. *Am J Pathol* 2002; **160**: 681–92.
32 Lechner JF, LaVeck MA, Gerwin BI *et al.* Differential responses to growth factors by normal human mesothelial cultures from individual donors. *J Cell Physiol* 1989; **139**: 295–300.
33 Wang Y, Faux SP, Hallden G *et al.* Interleukin-1beta and tumour necrosis factor-alpha promote the transformation of human immortalised mesothelial cells by erionite. *Int J Oncol* 2004; **25**: 173–8.
34 Choe N, Tanaka S, Xia W *et al.* Pleural macrophage recruitment and activation in asbestos-induced pleural injury. *Environ Health Perspect* 1997; **105** (Suppl 5): 1257–60.
35 Viallat JR, Raybuad F, Passarel M *et al.* Pleural migration of chrysotile fibers after intratracheal injection in rats. *Arch Environ Health* 1986; **41**: 282–6.
36 Kohyama N, Suzuki Y. Analysis of asbestos fibers in lung parenchyma, pleural plaques, and mesothelioma tissues of North American insulation workers. *Ann N Y Acad Sci* 1991; **643**: 27–52.
37 Miserocchi G, Sancini G, Mantegazza F *et al.* Translocation pathways for inhaled asbestos fibers. *Environ Health* 2008; **7**: 4.
38 NIOSH. Occupational exposure to carbon nanotubes and nanofibers. *Curr Intelligence Bull* 2010; **161-A**: 1–149.

Supporting Information

Additional Supporting Information may be found in the online version of this article:

Fig. S1. Characterization of multi-walled carbon nanotubes and crocidolite fibers in the suspensions.
Fig. S2. SEM observation of multi-walled carbon nanotubes and crocidolite fibers in the visceral pleura.
Fig. S3. Inflammation and fibrosis in the lung.
Fig. S4. Cytotoxicity of multi-walled carbon nanotubes and crocidolite to TCC-MESO1 cells *in vitro*.

doi: 10.1111/cas.12005

The Journal of Toxicological Sciences (J. Toxicol. Sci.)
Vol.39, No.2, 363-370, 2014

Original Article

Teratogenicity of asbestos in mice

Tomoko Fujitani[1], Motoki Hojo[1], Akiko Inomata[1], Akio Ogata[1], Akihiko Hirose[2], Tetsuji Nishimura[3] and Dai Nakae[1]

[1]Department of Pharmaceutical and Environmental Sciences, Tokyo Metropolitan Institute of Public Health, 3-24-1, Hyakunincho, Shinjuku-ku, Tokyo 169-0073, Japan
[2]Division of Risk Assessment, Biological Safety Research Center, National Institute of Health Science, 1-18-1, Kamiyoga, Setagaya-ku, Tokyo 158-8501, Japan
[3]Department of Pharmacology, Teikyo Heisei University, 4-21-2, Nakano, Nakano-ku, Tokyo 164-8530, Japan

(Received January 14, 2014; Accepted February 14, 2014)

ABSTRACT — Possible teratogenicity of 3 different asbestos (crocidolite, chrysotile and amosite) was assessed in CD1(ICR) mice. Dams on day 9 of gestation were given a single intraperitoneal administration at dose of 40 mg/kg body weight of asbestos suspended in 2% sodium carboxymethyl cellulose solution in phosphate buffered saline, while dams in the control group were given vehicle (10 ml/kg body weight). Dams and fetuses were examined on day 18 of gestation. To compare with the control group, the mean percentage of live fetuses in implantations in the group given crocidolite and the incidence of dams with early dead fetuses in the groups given chrysotile or amosite were increased. While no external or skeletal malformation was observed in the control group, the incidence of external malformation (mainly reduction deformity of limb) in the group given amosite, and the incidences of skeletal malformation (mainly fusion of vertebrae) in the all dosed groups were significantly increased. The result indicated that asbestos (crocidolite, chrysotile and amosite) have fetotoxicity and teratogenicity in mice.

Key words: Teratogenicity, Asbestos, Crocidolite, Chrysotile, Amosite, Mice

INTRODUCTION

In the 20th century, asbestos had been widely utilized as a heat-proofing, fire-proofing and insulating material for inner coating of buildings and ships or in the electrical products. From late 1960's, hazards of asbestos became evident in humans (Selikoff and Hammond, 1968; Sheers and Templeton, 1968; Knox *et al.*, 1968) and experimental animals (Shin and Firminger, 1973; Pott *et al.*, 1974). The asbestos exposure induced lung fibrosis, lung cancer and, especially, delayed malignant mesothelioma not only in the workers of industries dealing with asbestos by the occupational exposure but also in the family members of such workers by the domestic exposure (Wasserman *et al.*, 1980; Miller, 1979). In Japan, the manufacture of asbestos fibers and of products used asbestos was prohibited, with some special exceptions, in 2006 and was completely prohibited in 2011 by the Ministry of Health, Labor and Welfare of Japan. However, the sufferers from asbestosis may increase even in the future, because the malignant mesothelioma development by asbestos exposure has a long latency (20-55 years) in humans. And the great attention should be paid regarding on hazards of asbestos in the dust that will be released during the demolition of buildings and ships lined by asbestos in the past.

Recently, the induction of mesothelioma by multi-wall carbon nanotubes (MWCNT), a non-mineral asbestos-like fiber, has been reported in mice (Takagi *et al.*, 2008) and rats (Sakamoto *et al.*, 2009). Since then, the similarity and difference of carcinogenic events induced by those exogenous fibers have been enthusiastically discussed (Donaldson *et al.*, 2010; Schinwald *et al.*, 2012). On the other hand, during the course of toxicological evaluation for MWCNT, we have revealed the teratogenicity of MWCNT given intraperitoneally or intratracheally to mice (Fujitani *et al.*, 2012). And we are strongly interested in the possible teratogenicity of other fibrous materials, especially of asbestos, because the transplacental transfer of asbestos fibers into embryos were evident in humans and experimental animals (Cunningham and Pontefract, 1974; Haque *et al.*, 1992, 1998 and 2001;

Correspondence: Tomoko Fujitani (E-mail: Tomoko_Fujitani@member.metro.tokyo.jp)

Haque and Vrazel, 1998). To the best of our knowledge, there are no data available so far in the literature to describe either the presence or absence of the teratogenicity of asbestos. In this context, the present study was carried out to assess possible teratogenicity of asbestos, crocidolite, chrysotile and amosite, in mice.

MATERIALS AND METHODS

Ethical consideration of the experiment

An experimental protocol was approved by the Experiments Regulation Committee and the Animal Experiment Committee of the Tokyo Metropolitan Institute of Public Health prior to its execution and monitored at every step during the experimentation for its scientific and ethical appropriateness, including concern for animal welfare, with strict obedience to the National Institutes of Health Guideline for the Care and Use of Laboratory Animals, Japanese Government Animal Protection and Management Law, Japanese Government Notification on Feeding and Safekeeping of Animals and other similar laws, guidelines, rules *et cetera* provided domestically and internationally.

Test chemicals

Crocidolite, chrysotile and amosite (all chemically pure and pretreated Union Internationale Centre le Cancer (UICC)), were autoclaved (120°C, 30 min) for the sterility and were suspended in sterilized 2% sodium carboxymethyl cellulose (Tokyo Chemical Industry Co., Ltd., Tokyo, Japan) /phosphate buffered saline by vigorous stirring and sonication, to gain the uniform suspension.

Animals

Specific pathogen free female Crlj: CD1(ICR) mice, on gestational days 3, 4, 7 or 8 (the day with vaginal plug at the morning after housing with male was regarded as day 0), were purchased from Charles River Japan Inc. (Kanagawa, Japan) and were housed individually in plastic cages with cedar chip bedding and allowed free access to the standard diet CE2 (Nihon Clea, Inc., Tokyo, Japan) and water. The animal room was maintained at 23-25°C with a relative humidity of 50-60%, with 10 ventilations per hour (drawing fresh air through an HEPA-filter, 0.3 μm, 99.9% efficiency) and on a 12 hr light/dark cycle.

Experiment

On day 9 of gestation, dams were randomly allocated to 4 groups by body weights and were given a single intraperitoneal administration of asbestos at the dose of 40 mg/10 ml/kg body weight. The control mice were given vehicle. Body weights and food consumptions were measured daily and clinical observations were recorded. Relative food consumptions were calculated by dividing the absolute food consumption by the body weight (g/kg body weight/day). On day 18 of gestation, dams were anesthetized by diethyl ether and blood samples were collected in EDTA2K-anticoagulant tubes from the femoral vein. The white blood cell counts were examined by an auto-blood analyzer SYSMEX KX21-NV (SYSMEX, Kobe, Japan). Blood films were made, stained by Diff-Quik (SYSMEX) and counted for the subtypes of white blood cells under the light microscopy. Livers, kidneys, spleens and adrenals of dams were weighed. Uteri were opened, and the numbers and positions of implantation sites, early dead fetuses (defined as a case showing the implanted site and amorphous mass), late dead fetuses (defined as a case showing head and limbs) and live fetuses were examined. The numbers of corpora lutea in ovaries were also examined. Each live fetus was weighed and examined for external anomalies. Fetuses, of which internal organs in the peritoneal and thoracic cavities were carefully removed, were fixed in 95% ethanol for more than 1 week, soaked in 0.5% KOH for 24 hr, in 0.002% Alizarin Red S/ 0.5% KOH for 24 hr, in 0.4% KOH/20% Glycerin for 24 hr, in 50% Glycerin for more than 24 hr and examined for skeletal anomalies.

Statistical analysis

Scheffe's multiple comparison was applied for body weight of dam, food consumption of dam, number of implantations, number of early or late dead fetuses, number of live fetuses, and mean fetal body weights in each dam. The incidence of dams with early dead fetuses, late dead fetuses or malformed fetuses in dams in the groups and the incidence of malformed fetuses in the fetuses in the group were analyzed using the Chi square test.

RESULT

Dams did not die from the administration of asbestos in the current experimental conditions. Body weights of dams on 1 to 2 days after the administration of crosidolite, on 1 to 5 days after the administration of chrysotile, on 1 day after administration of amosite were significantly lower than that of the control group (Fig. 1). Absolute and relative food consumptions on 1 day after the administration of crocidolite, chrysotile and amosite were significantly lower than that of the control group (data not shown). Immediately after the administration to about 1

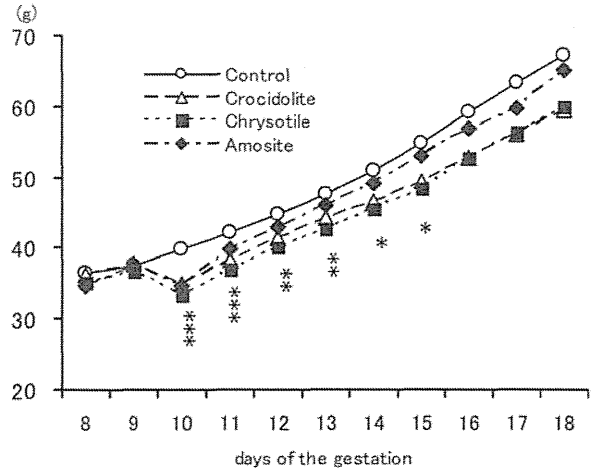

Fig. 1. Body weight gains of dams.

day after, dams given asbestos seemed less active than those of the control group. Effects of asbestos on dams are summarized in Table 1. Liver and spleen weight of dams in the group given crocidolite or amosite were significantly higher than those of the control group, while weights of kidneys and adrenals were not changed by administration of asbestos. The total white blood cell counts and the neutrocyte counts of dams in the group given crocidolite or amosite were significantly higher than that of the control group. In addition, monocyte counts of dams in the group given amosite was also significantly higher than that of the control group.

Pregnant statuses of dams are presented in Table 2. Most of the mated mice were gestated and had living fetuses regardless to the administration of asbestos. There was no statistical difference between control and dosed groups on the numbers of corpora lutea, implantation sites, early or late fetal death and live fetuses. However, the incidence of dams with early dead fetuses in groups given chrysotile or amosite was significantly increased to compare with that of the control group. Also, the percentage of live fetuses in the implantation sites of the group given crocidolite was significantly lower than that of the control group. The incidence of dams with late dead fetuses was not changed by administration of asbestos. Body weight of live fetuses (male and female) was not changed by administration of asbestos.

Incidences of malformation are presented in Table 3. The incidences of dams with fetuses having external malformations and the incidences of fetuses with external malformations were both significantly increased in the group given amosite. Observed external malformations included cleft face (Fig. 2), reduction deformity of limb (absence of finger or of forelimb) (Fig. 3), omphalocele, absent genital tubercule and absent tail (Fig. 4). Among those malformations, the incidence of the reduction deformity of limb significantly increased in the group

Table 1. Effects of intraperitoneal dose of asbestos on dams.

	Control	Asbestos dosed (40 mg/kg b.w.)		
	(CMCNa)	Crocidolite	Chrysotile	Amosite
Number of dams	9	10	9	10
Body weight (g) on day 9 of gestation	37.48 ± 2.07	37.89 ± 1.06	36.64 ± 1.75	37.64 ± 1.97
on day 18 of gestation	67.04 ± 6.02	59.54 ± 8.73	60.02 ± 6.92	65.14 ± 8.23
Organ weight				
Liver (g)	3.00 ± 0.24	3.83 ± 0.53***	3.41 ± 0.18	3.90 ± 0.32***
Kidney (mg)	458 ± 54	490 ± 51	441 ± 61	500 ± 21
Spleen (mg)	137 ± 20	422 ± 206***	266 ± 72	418 ± 126***
White blood cell count (10^2/μl)				
Total	42.5 ± 11.1	85.5 ± 31.4*	74.9 ± 19.5	101.5 ± 31.0***
Lymphocyte	31.7 ± 8.8	29.5 ± 10.1	30.2 ± 6.3	28.0 ± 6.7
Neutrocyte	9.6 ± 3.4	47.9 ± 21.7**	33.1 ± 12.2	64.0 ± 25.8***
Eosinocyte	0.4 ± 0.4	3.6 ± 3.0	7.4 ± 6.5	3.8 ± 2.1
Monocyte	0.8 ± 0.2	4.5 ± 3.4	4.2 ± 3.0	5.6 ± 3.3*

Values are the means ± standard deviations for numbers of dams in each group. Asterisks represent that the values are significantly different from the corresponding control values (*, ** or *** indicating $p < 0.05$, 0.01 or 0.001, respectively).

Table 2. Pregnant status of mice given Asbestos intraperitoneally on day 9 of the gestation

Reproductive parameters	Control	Asbestos dosed (40 mg/kg b.w.)		
	(CMCNa)	Crocidolite	Chrysotile	Amosite
Females mated[1)]	10	10	10	10
Females gestated[2)]	9	10	9	10
Females with >1 live fetus	9	10	9	10
Corpora lutea/litter[#]	17.9 ± 1.8	19.3 ± 1.4	18.7 ± 1.3	18.5 ± 1.4
Implantations/litter[#]	14.6 ± 2.5	14.3 ± 1.6	14.2 ± 1.2	14.9 ± 1.4
Death of fetuses[3)#]				
Number of early dead fetuses	0.1 ± 0.3	5.1 ± 5.5	3.9 ± 4.3	3.2 ± 3.3
(% of implantations)	(0.9 ± 2.8)	(36.2 ± 38.9)	(26.5 ± 28.6)	(22.0 ± 23.2)
Females with early dead fetuses/examined	1/9	5/10	8/9**	8/10**
Number of late dead fetuses	0	0.2 ± 0.4	0	0.1 ± 0.3
(% of implantations)	(0.0)	(1.4 ± 3.0)	(0.0)	(0.7 ± 2.1)
Females with late dead fetuses/examined	0/9	2/10	0/9	1/10
Live fetuses/litter[#]	14.4 ± 2.7	9.2 ± 5.3	10.3 ± 3.9	11.6 ± 3.7
(% of implantations)	(99 ± 3)	(64 ± 36*)	(74 ± 29)	(77 ± 23)
Body weight of live fetuses (g)[#]				
Male	1.47 ± 0.08	1.42 ± 0.12	1.43 ± 0.04	1.39 ± 0.08
Female	1.39 ± 0.08	1.33 ± 0.09	1.35 ± 0.06	1.33 ± 0.08

[1)] Number of animals with vaginal plug.

[2)] Number of animals with implantation sites.

[3)] 'Early' was defined as a case showing the implanted sites and amorphous mass, while 'Late' was defined as a case showing the head and limbs.

[#] Values are the means ± standard deviations.

The percent resorption (early or late dead fetus) and fetal body weight were obtained by averaging the value for each litter.

Asterisks represent that the values are significantly different from the corresponding control values (*, ** or *** indicating $p < 0.05$, 0.01 or 0.001, respectively).

given amosite. One reduction deformity (lack of a finger) in the group given crocidolite and one open eyelid in the group given chrysotile were observed but there was no statistical significance in the increase of those incidences. The incidences of dams with fetuses having skeletal malformations in the group given chrysotile and amosite were significantly increased compared with the control group. The incidences of fetuses with skeletal malformations in the all groups given asbestos were significantly increased compared with that of the control group. Among the observed skeletal malformations, the incidence of fusion of vertebral bodies and arches (Fig. 5) in the all groups given asbestos were significantly increased. Also, the incidence of reduction deformity of limb (absence of finger bones, absence of arm bone and so on) in the group given amosite was statistically significant.

DISCUSSION

The intraperitoneal administration of crocidolite, chrysotile and amosite had teratogenic effects in mice. We conducted the experiment of administration in intraperitoneal cavity to avoid the stress to the dam in the intratracheal administration. However, the fact that intraperitoneal administration of MWCNT had equal teratogenicity to that of the intratracheal administration (Fujitani *et al.*, 2012) led to the potential teratogenicity of those asbestos in the intratracheal exposure. The dose level in the present experiment on asbestos was over 10-fold higher compared with that on MWCNT (Fujitani *et al.*, 2012) as based on the weight of substance tested. The asbestos are mineral fibers having density at 2.4 to 3.25 g/cm^3. In contrast, MWCNT, having inner diameter of 2-10 nm as a cylinder form of graphene sheet having vacant inner space, has a bulk density at 0.14 to 0.28 g/cm^3. So, the bulk of 4 mg

Table 3. Incidences of malformations in mice given asbestos on day 9 of gestation

	Control	Asbestos dosed (40 mg/kg b.w.)		
	(CMCNa)	Crocidolite	Chrysotile	Amosite
External malformation				
Number of litters with malformed fetus/examined (percentages in the parentheses)				
	0/9 (0)	1/10 (10)	1/9 (11)	4/10 (40)*
Percent incidence of malformations#	0	2.0 ± 6.3	0.9 ± 2.8	4.1 ± 5.5
Numbers of malformed fetuses/examined	0/130	1/92	1/93	5/116*
Numbers of fetuses with				
open eyelid	0	0	1	0
cleft face	0	0	0	1
reduction deformity of limb	0	1	0	4*
omphalocele	0	0	0	1
absent genital tubercle	0	0	0	1
absent tail	0	0	0	1
Skeletal malformation				
Number of litters with malformed fetuses/examined (percentages in the parentheses)				
	0/9 (0)	3/10 (30)	4/9 (44)*	7/10 (70)**
Percent incidence of malformations#	0	7.4 ± 12.0	11.2 ± 18.1	10.5 ± 8.6
Numbers of malformed fetuses/examined	0/130	6/92**	5/93**	13/116***
Numbers of fetuses with				
gnatho-dysplasia	0	0	0	1
fusion of vertebral body and arch	0	5**	5**	9**
fusion of rib	0	2	1	1
reduction deformity of limb	0	1	0	6**
kinked or absent tail	0	0	2	1

Values are the means ± standard deviations obtained by averaging the value for each dam.
Asterisks represent that the values are significantly different from the corresponding control values (*, ** or *** indicating $p < 0.05$, 0.01 or 0.001, respectively).

MWCNT was shown to be equal to the bulk of 40 mg asbestos fibers (Fig. 6). In the preliminary study on teratogenicity of asbestos, we did not observe any adverse effects of asbestos on dam and fetus in the dose level of 4 mg/kg body weight and the bulk of 4 mg of asbestos seems very little to compare with the 4 mg MWCNT (Fig. 7). The detailed dose-dependent profile of the teratogenicity of asbestos is now being assessed in our laboratories.

Winkler and Rüttner (1982) reported that numerous phagocytes were mobilized on the surface of the mesenteric tissue to engulf asbestos fibers given intraperitoneal cavity within 24 hr. We observed the grayish-colored and/or swollen lymph nodes beside the thymus in thoracic cavity of dams given asbestos (data not shown) in the same way observed in dams given MWCNT. It is thus likely to speculate that intraperitoneally administered asbestos fibers in the present study might at least partly be carried by lymphatic or blood flow from peritoneal cavity. Some literature indicates that transplacental distribution of asbestos from dam to fetus (Cunnibgham and Pontecraft, 1974; Haque *et al.*, 1992, 1998 and 2001; Haque and Vrazel 1998). So, asbestos fibers might penetrate past the placenta to embryos in the present study. As asbestos have cytotoxicity (Lipkin, 1980; Lock and Chamberlain, 1983) and genotoxicity (Libbus *et al.*, 1989; Marczynski *et al.*, 1994; Dopp *et al.*, 1997; Dopp and Schiffmann, 1998) on mammalian cells, rapidly proliferating embryonic cells may become an essential target of the asbestos toxicity. The result that the administration of chrysotile and amosite increased the

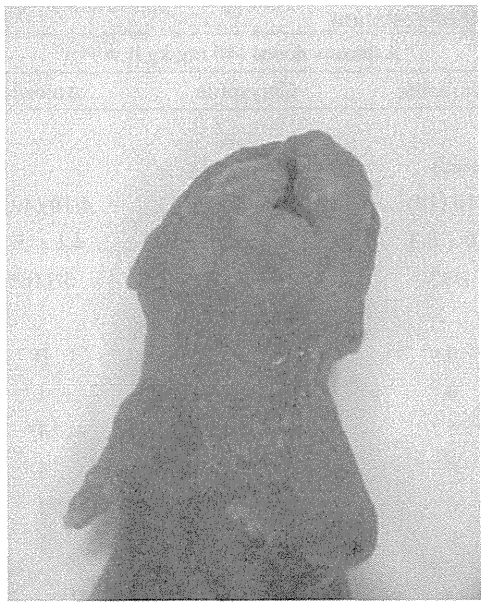

Fig. 2. Cleft face and reduction deformity of right forelimb shown in a fetus of the group given amosite.

Fig. 3. Reduction deformity of right and left forelimbs shown in a fetus of the group given amosite.

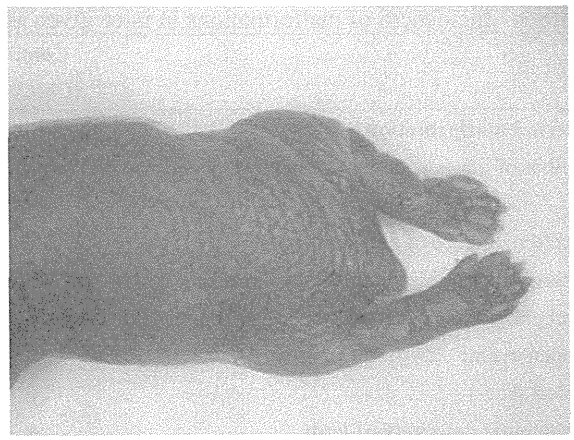

Fig. 4. Absence of tail shown in a fetus of the group given amosite.

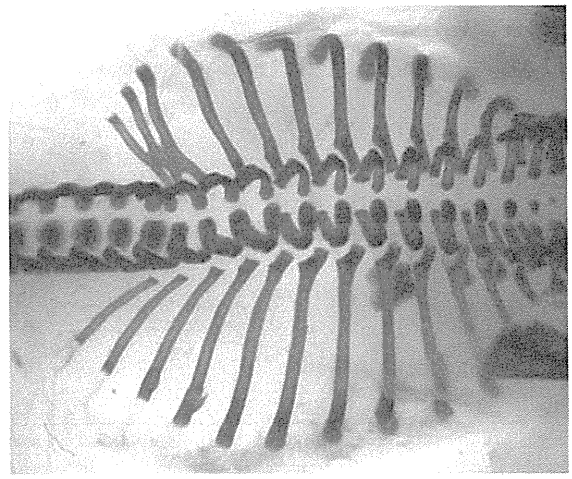

Fig. 5. Fusion of vertebrae and ribs shown in a fetus of the group given crocidolite.

incidence of dams with early dead fetus and the administration of crosidolite decreased the percentages of live fetuses in the implantation sites indicated the lethal damage(s) by asbestos on whole embryos. And, in the surviving fetuses, external and/or skeletal malformations were evident in the groups given asbestos. Gestational day 9 is the specific narrow window to cause the reduction deformity of limbs and tail in fetuses of mice given teratogenic chemicals (Ogata *et al.*, 1984). Although asbestos fibers were still observed macroscopically in the peritoneal cavity on day 18 of gestation, the adverse effect of asbestos on fetuses appeared to be restricted in the early stage of the organogenesis period, because late fetal death and weight of fetuses were not changed in the groups given asbestos. Another possible pathogenesis of exogenous fibers may be immuno-modulating and inflammatory effects. Pleural inflammation was targeted regarding on induction of mesothelioma by carbon nanotubes (Murphy *et al.*, 2012) and asbestos (Schinwald *et al.*, 2012). Yamaguchi *et al.* (2012) reported the stimulated immune and inflammatory responses from 1 to 20 weeks after intraperitoneal administration of MWCNT in female mice. In that study, effects of crocidolite were also examined to compare with those of MWCNT and the admin-

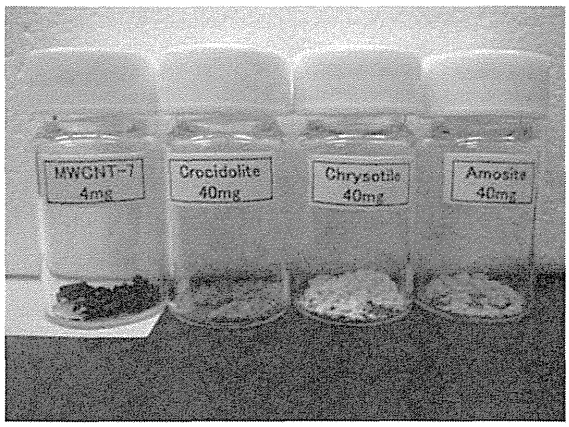

Fig. 6. Macroscopic appearance of Asbestos (40 mg) and MWCNT (4 mg).

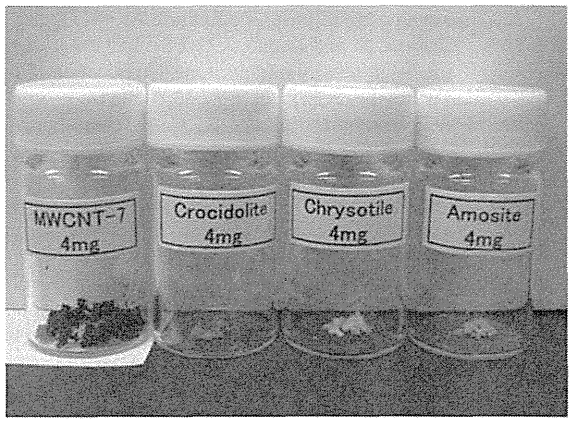

Fig. 7. Macroscopic appearance of Asbestos (4 mg) and MWCNT (4 mg).

istration of crocidolite fibers significantly increased the white blood cell counts, granulocyte counts and monocyto counts in peripheral blood at 1 week after the administration. In the present study, white blood cell counts were tended to increase in all the groups given asbestos, even though statistical significance was not apparent in the group given chrysotile. And the result of the present study indicated that the increase of white blood cell counts in dosed groups were due to the increase of neutrocyte counts. There was a tendency to increase eosinocyte counts and monocyte counts in the dosed groups but statistical significance was evident only in the monocyte counts in the amosite group. So, most striking change in white blood cell counts of dam given asbestos was the increase of neutrocytes. The relation between the immunological changes in dam and the defects of embryonal development is unclear at present. However, the splenomegaly shown in dams given asbestos in the present study and MWCNT (Fujitani *et al.*, 2012) indicated the disturbance of immunological and/or hematological system(s) in those dams. We weighed the main organ weight (liver, kidney and spleen) to monitor the general damages in dams given asbestos. The increase of liver weight, having significance in the groups given crocidolite and amosite or tendency in the group given chrysotile, possibly indicated acute effects on the liver by asbestos. The pathological examination on livers and spleens of those dams is under progress in our laboratory.

Further study might be required, including experiments by other administration routes, for example, intratracheal or oral which may be valuable to clarify the non-hazardous dose of teratogenic effects of asbestos in humans.

ACKNOWLEDGEMNTS

This work was supported in part by a research budget of the Tokyo Metropolitan Government, Japan, and a Grant-in-Aid from the Ministry of Health, Labor and Welfare of Japan. The authors gratefully thank to Mr. Ando and Mr. Kubo for their technical assistance, Dr. Hiraga, the founder of the department of toxicology in our institute, and Dr. Yoneyama, for her effort to open the door to the toxicologist for the first author.

REFERENCES

Cunningham, H.M. and Pontefract, R.D. (1974): Placental transfer of asbestos. Nature, **249**, 177-178.

Donaldson, K., Murphy, F.A., Duffin, R. and Poland, C.A. (2010): Asbestos, carbon nanotubes and the pleural mesothelium: A review of the hypothesis regarding the role of long fibre retention in the parietal pleura, inflammation and mesothelioma. Part Fibre. Toxicol., **7**, 5.

Dopp, E., Schuler, M., Schiffmann, D. and Eastmond, D.A. (1997): Induction of micronuclei, hyperdiploidy and chromosomal breakage affecting the centric/pericentric regions of chromosomes 1 and 9 in human amniotic fluid cells after treatment with asbestos and ceramic fibers. Mutat. Res., **377**, 77-87.

Dopp, E. and Schiffmann, D. (1998): Analysis of chromosomal alterations induced by asbestos and ceramic fibers. Toxicol. Lett., **96-97**, 155-162.

Fujitani, T., Ohyama, K., Hirose, A., Nishimura, T., Nakae, D. and Ogata, A. (2012): Teratogenicity of multi-wall carbon nanotube (MWCNT) in ICR mice. J. Toxicol. Sci., **37**, 81-89.

Haque, A.K., Mancuso, M.G., Williams, M.G. and Dodson, R.F. (1992): Asbestos in organs and placenta of five stillborn infants suggests transplacental transfer. Environ. Res., **58**, 163-175.

Haque, A.K. and Vrazel, D.M. (1998): Transplacental transfer of asbestos in pregnant mice. Bull. Environ. Contam. Toxicol., **60**, 620-625.

Haque, A.K., Vrazel, D.M. and Uchida, T. (1998): Assessment of

asbestos burden in the placenta and tissue digests of stillborn infants in South Texas. Arch. Environ. Contam. Toxicol., **35**, 532-538.

Haque, A.K., Ali, I. and Vrazel, D.M. (2001): Chrysotile asbestos fibers detected in the newborn pups following gavage feeding of pregnant mice. J. Toxicol. Environ. Health, Part A, **62**, 23-31.

Knox, J.F., Holmes, S., Doll, R. and Hill, I.D. (1968); Mortality from lung cancer and other causes among workers in an asbestos textile factory. Br. J. Ind. Med., **25**, 293-303.

Libbus, B.L., Illenye, S.A. and Craighead, J.E. (1989): Induction of DNA strand breaks in cultured rat embryo cells by crocidolite asbestos as assessed by nick translation. Cancer Res., **49**, 5713-5718.

Lipkin, L.E. (1980): Cellular effects of asbestos and other fibers: Correlations with *in vivo* induction of pleural sarcoma. Environ. Health Perspect., **34**, 91-102.

Lock, S.O. and Chamberlain, M. (1983): Cytotoxic action of mineral dusts on CHV 79 cells *in vitro*: Factors affecting toxicity. Environ. Health Perspect., **51**, 189-193.

Marczynski, B., Czuppon, A.B., Marek, W. Reichel, G. and Baur, X. (1994): Increased incidence of DNA double-strand breaks and anti-ds DNA antibodies in blood of workers occupationally exposed to asbestos. Hum. Exp. Toxicol., **13**, 3-9.

Murphy, F.A., Schinwald, A., Poland, C.A. and Donaldson, K. (2012): The mechanism of pleural inflammation by long carbon nanotubes: interaction of long fibres with macrophages stimulates them to amplify pro-inflammatory responses in mesothelial cells. Particle and Fibre Toxicology, **9**, 8.

Miller, R.W. (1979): Advances in understanding causes of childhood cancer. Pediatric Analis., **8**, 710-715.

Ogata, A., Ando, H., Kubo, Y. and Hiraga, K. (1984): Teratogenicity of thiabendazole in ICR mice. Food Chem. Toxic., **22**, 509-520.

Pott, F., Huth, F. and Friedrichs, K.H. (1974): Tumorigenic effect of fibrous dusts in experimental animals. Environmental Health Perspectives, **9**, 333-315.

Sakamoto, Y., Nakae, D., Fukumori, N., Tayama, K., Maekawa, A., Imai, K., Hirose, A., Nishimura, T., Ohashi, N. and Ogata, A. (2009): Induction of mesothelioma by a single intrascrotal administration of multi-wall carbon nanotube in intact male Fischer 344 rats. J. Toxicol. Sci., **34**, 65-76.

Schinwald, A., Murphy, F.A., Prina-Mello, A., Poland, C.A., Byrne, F., Movia, D., Glass, J.R., Dickerson, J.C., Schultz, D.A., Jeffree, C.E., MacNee, W. and Donaldson, K. (2012): The threshold length for fiber-induced acute pleural inflammation: Shedding light on the early events in asbestos-induced mesothelioma. Toxicol. Sci., **128**, 461-470.

Schneider, U. and Maurer, R.R. (1977): Asbestos and embryonic development. Teratology, **15**, 273-279.

Selikoff, I.J. and Hammond, E.C. (1968): Environmental epidemiology. 3. Community effects of nonoccupational environmental asbestos exposure. Am. J. Public Health Nations Health, **58**, 1658-1666.

Sheers, G. and Templeton, A.R. (1968): Effects of asbestos in dockyard workers. Br. Med. J., **3**, 574-579.

Shin, M.L. and Firminger, H.I. (1973): Acute and chronic effects of intraperitoneal injection of two types of asbestos in rats with a study of the histopathogenesis and ultrastructure of resulting mesotheliomas. Am. J. Pathol., **70**, 291-314.

Takagi, A., Hirose, A., Nishimura, T., Fukumori, N., Ogata, A., Ohashi, N., Kitajima, S. and Kanno, J. (2008): Induction of mesothelioma in p53+/- mouse by intraperitoneal application of multi-wall carbon nanotube. J. Toxicol. Sci., **33**, 105-116.

Wasserman, M., Wasserman, D. Steinitz, R., Katz, L. and Lemesch, C. (1980): Mesothelioma in children. IARC Sci. Publ., **30**, 253-257.

Winkler, G.C. and Ruttner, J.R. (1982); Penetration of asbestos fibers in the visceral peritoneum of mice. A scanning electron microscopic study. Exp. Cell Biol., **50**, 187-194.

Yamaguchi, A., Fujitani, T., Ohyama, K., Nakae, D., Hirose, A., Nishimura, T. and Ogata, A. (2012): effects of sustained stimulation with multi-wall carbon nanotubes on immune and inflammatory responses in mice. J. Toxicol. Sci., **37**, 177-189.

<研究最前線>

液ー液界面析出法によるフラーレンナノファイバーの合成と成長機構

Synthesis of fullerene nanofibers by liquid-liquid interfacial precipitation method and their growth mechanism

Various forms of fullerene nanofibers have been synthesized since the discovery of C_{60} nanowhiskers (C_{60}NWs) in 2001. Among them, C_{60}NWs have been most minutely investigated for their physicochemical properties and applications for transistors and sensors. In 2011, we succeeded in the synthesis of superconducting C_{60}NWs by doping potassium. The investigation of growth mechanism is a key theme for the practical applications of fullerene nanofibers including the superconductivity. This paper reviews the recent growth study of C_{60}NWs and discusses the growth mechanism of C_{60}NWs.

独立行政法人物質・材料研究機構　先端材料プロセスユニット
フラーレン工学グループ
Fullerene Engineering Group, Materials Processing Unit,
National Institute for Materials Science

宮澤　薫一
Kun'ichi Miyazawa

1. はじめに

フラーレンナノファイバーとは、C_{60}分子、C_{70}分子、$(\eta^2\text{-}C_{60})Pt(PPh_3)_2$や$C_{60}[C(COOC_2H_5)_2]$のようなフラーレンの誘導体、$Sc_3N@C_{80}$のような元素内包フラーレンなどあらゆるフラーレン分子及びその誘導体から構成される細い繊維状物質であり、それらの直径は 1,000 nm 未満として定義されている[1]。フラーレンナノファイバーは単結晶、多結晶、非晶質構造のあらゆるものが許される。フラーレンナノウィスカーとは、フラーレンナノファイバーの一種であり、単結晶状かつ中空でない針状結晶を指す。ウィスカーとは細長い針状結晶（ひげ結晶）のことであり、また特に、中空なフラーレンナノファイバーをフラーレンナノチューブと呼んでいる。Fig.1 に今日まで合成された様々なフラーレンナノファイバーを示す。

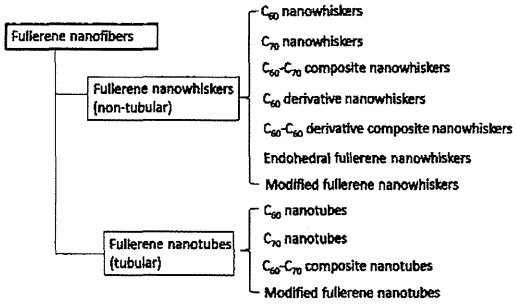

Fig.1. Fullerene nanofibers synthesized till today.

フラーレンナノファイバーの内で最も良く研究されて来たものは、C_{60}分子から構成される C_{60} ナノウィスカー（C_{60}NW）である。C_{60}NW は、チタン酸ジルコン酸鉛（PZT）の薄膜をゾル・ゲル法によって合成する際に焼成温度を下げることを目的として少量の C_{60} を添加する実験で見出された[2]。2002 年には、フラーレン

宮澤　薫一
（独）物質・材料研究機構 先端材料プロセスユニット フラーレン工学グループリーダー 工学博士
〒305-0044 茨城県つくば市並木 1-1
1979 年 東京大学農学部林学科卒業、1981 年 同教養学部基礎科学科卒業、1985 年 同大学院工学系研究科博士課程退学
専門：材料工学
E-mail：miyazawa.kunichi@nims.go.jp

ナノファイバーの標準的合成法である液－液界面析出法（liquid - liquid interfacial precipitation (LLIP) method"を発表した[3]。

純粋なC_{60}結晶のヤング率は約20GPaであるが[4]、透過電子顕微鏡(TEM)によるその場測定では、C_{60}NW は 32～54GPa の高い値を示した[5]。この場合、電子線照射によってC_{60}分子が重合することが知られているので[6]、電子線重合によってC_{60}NW のヤング率が 2 倍以上に増加したことが推察される。一方、C_{60}分子は紫外光や可視光によっても重合することが知られていたが [7]、C_{60}NW においても緑色レーザー光によってC_{60}分子が重合することが見出された[8]。合成直後の C_{60}NW の破断応力は 7.7MPa であった[9]。これは純粋な C_{60} 結晶の降伏応力 0.7MPa の約 10 倍の値であるが[10]、光や電子線照射によってC_{60}分子の重合度を高めれば、より高強度の C_{60}NW を得ることができると期待される。

アルカリ金属を添加することによってC_{60}NW が超伝導を示すことが予想されていたが[11、12]、2011 年、カリウム(K)を添加することにより C_{60}NW を超伝導化することに成功した[13]。この場合の超伝導転移温度 T_cは 17K であった。1991 年に K 添加 C_{60}結晶が超伝導体(超伝導転移温度 T_c=18K)となることが発見されてより[14]、多数のフラーレン超伝導化研究が行われた。常圧環境では、セシウム(Cs)とルビジウム(Rb)を添加した $Cs_2Rb_1C_{60}$ が最高の Tc=33K を示す[15]。そのため、$Cs_2Rb_1C_{60}$ 組成の C_{60}NW も、33K 近くの T_cを持つ超伝導体となることが予想される。

フラーレンナノウィスカー(FNW)超伝導体のメリットは、密度が約 2gcm^{-3} 程度で金属やセラミックス超伝導体に比べて格段に軽いこと、もともとファイバー形状であるため電送ケーブルのような線材の作製に適していること、使用後は有機溶媒で溶解させてフラーレンを回収することができること、カリウムやフラーレンを構成する炭素は多量に存在し資源的に問題がないこと等であり、また、C_{60}NW の細胞毒性が多層カーボンナノチューブやチタニアナノ粒子に比べて低いと報告されていることも実用的に重要な事項である[16]。将来、多様な超伝導フラーレンナノファイバーが誕生すると予想されるが、軽量でしなやかな特徴を生かした用途開発、例えば、軽い超伝導モータ・発電機、軽くしなやかな超伝導磁気シールド材・電送ケーブル等への利用が期待される。

超伝導利用のみならず、C_{60}NW と C_{60}ナノチューブ(C_{60}NT)は、電界効果トランジスタ[17、18、19]、太陽電池[20]、ドーパミン検出用のバイオセンサ[21]等、様々な応用研究が行われており、フラーレンナノファイバーは高い可能性を持つが、広く実用されるためには、形状を自由に制御できる技術を確立することが必要である。

そこで本稿では、フラーレンナノファイバーの合成方法とこれまでに明らかにされたC_{60}NW の成長機構について述べる。

2. 液－液界面析出法（LLIP 法）

液－液界面析出法（liquid-liquid interfacial precipitation method, LLIP 法）とは、フラーレンの良溶媒飽和溶液にフラーレンの貧溶媒を重層して液－液界面を作り、両溶媒の相互拡散とともに進行するフラーレン結晶核の生成と成長によりフラーレンナノファイバーを合成する方法である。良溶媒／貧溶媒の組合せとして、トルエン／イソプロピルアルコール(IPA)、メタキシレン／IPA、ピリジン／IPA の組合せの場合、C_{60}NW は溶液中では六方晶として成長し、乾燥によって溶媒を失うと結晶格子の組み変えが生じて面心立方晶(FCC)に変化する[22、 23、 24]。Table 1 に示すように、様々な溶媒の組合せによりフラーレンナノファイバーが合成されている。

Table.1. Combinations of good solvents and poor solvents used for the synthesis of various fullerene nanofibers.

Fullerene nanofibers	Good solvent	Poor solvent
C_{60} nanowhisker	toluene	IPA[3,8, 43]
	benzene	IPA[25,26,27]
	m-xylene	IPA[28]
C_{70} nanowhisker	toluene	IPA[29]
	m-xylene	IPA[28]
C_{70} nanotube	pyridine	IPA[30]
	pyridine	isobutyl alcohol [31]
C_{60}(nano)tube	pyridine	IPA[32,33,34,35, 43]
	benzene	1-butanol [36]
C_{60}-C_{70} two-component nanotube	pyridine	IPA[30]
$C_{60}[C(COOC_2H_5)_2]$ nanowhisker	toluene	IPA[37]
$Sc_3N@C_{80}$ nanowhisker	toluene, CS_2	IPA[38]

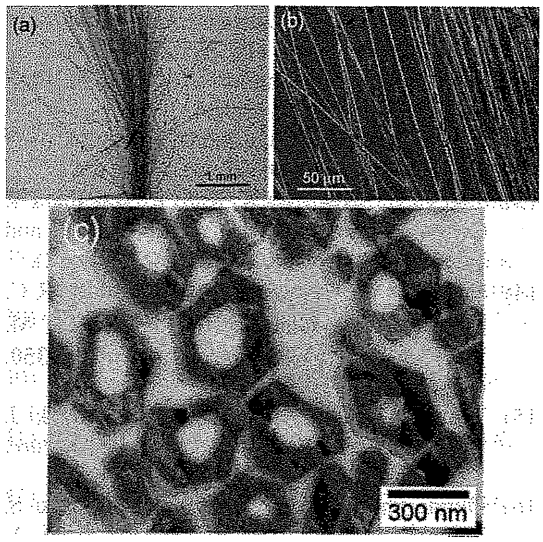

Fig.2. (a) Optical micrograph of as-prepared C_{60}NTs and (b) magnified image of the C_{60}NTs. (c)Cross-sectional TEM (200 kV) image for the C_{60}NTs. Reprinted with permission from [35].

Fig.2 は、C_{60}分子からなる中空なフラーレンナノファイバー＝C_{60} ナノチューブ(C_{60}NT)の合成例である。Fig.2(c)の断面透過電子顕微鏡像（断面 TEM 像）に示すように、C_{60}NT の断面形状は主として六角形であり、外径約 300nm の C_{60}NT の中央部に数 10nm から約 150nm 径の穴が開いているようすが分かる。この中空部に様々な物質を担持させることが可能である。

Fig.2(a)に示すように、C_{60}飽和ピリジン溶液と IPA の組合せにより、C_{60}NT は数 mm 以上の長さに容易に成長する。Fig.2(b)に示すように、C_{60}NT は途中で枝分かれすることなく、良い直線性を保って成長している。

C_{60}飽和トルエン／IPA の系では、C_{60}NW の成長の活性化エネルギーは 52.8 kJ/mol であった[39]。この値は、トルエンとアセトニトリル混合溶媒中における C_{60}の拡散の活性化エネルギー13.1 kJ/mol に比べて約 4 倍大きい。直接の比較は難しいが、C_{60}NW 成長の高い活性化エネルギーは、大きな脱溶媒和エネルギーが必要なためであると推察される。

LLIP 法は、液－液界面を形成後、そのまま静置しフラーレン結晶を成長させる方法（静置液－液界面析出法、Static LLIP 法）と、液－液界面を形成後、超音波照射、手振り混合や機械的混合等により意図的に界面を乱してフラーレン結晶の核生成と生長をさせる方法(変形液－液界面析出法、Modified LLIP 法)がある[40]。

C_{60}飽和メタキシレン溶液と静置液－液界面法により、長期間に C_{60}NW がどのように成長するかを調査した。5℃と 10℃の温度では、液－液界面形成後 5 日程度経過すると、界面が消失することが観察された。成長期間を 1～100 日として C_{60}NW の平均長の変化を調べたところ、長さは単調に増加するのではなく、増減を繰り返しながら増加することが明らかになった。

Fig.3 は、合成温度が 5℃と 10℃における C_{60}NW の平均長の変化を合成日数の関数としてプロットしたものである[41]。いずれの図も、初日に比べて 2 日目は長さが短くなり、3 日目にはより長くなり、しばらく経過すると短くなるというように、長さの増減を繰り返しつつ成長して行くようすを示しており、C_{60}NW の成長が、溶解と再析出を繰り返しながら進行することが分かる。また、5℃の場合に比べて 20℃の方が平均の成長速度が大きいことが分かる。合成温度が高い方が成長速度が大きいことは、C_{60}NW 飽和トルエン溶液と IPA を用いた実験においても認められている[39]。

C_{60}NW の成長には、温度と光の因子の他に、溶媒組成と水分も大きく影響することが明らかになった[40、42]。C_{60} 飽和トルエン溶液と IPA の系において、IPA に添加する水の量を、2.5mass%までの範囲で増加させると、増加量

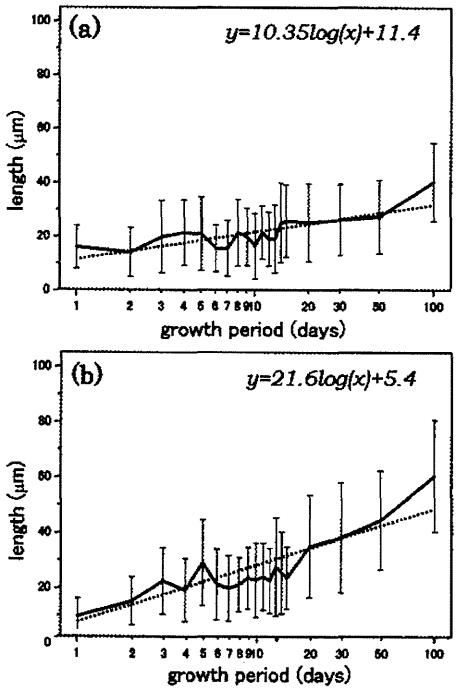

Fig.3. The length of C_{60}NWs plotted as a function of growth period. The growth temperature is (a) 5 °C and (b) 20 °C, respectively. Reprinted with permission from [41].

に応じて、直線的に C_{60}NW の長さが増加すること、また水の添加量の増加に伴って成長の活性化エネルギーが低下することが観察された[42]。しかし、過剰の水を添加すると C_{60}NW は不安定となり再溶解することが明らかになった[40]。このことは、C_{60}NW が水環境中では不安定であり、生物内耐久性でないことを示唆する。

3. まとめ

C_{60}NW の成長には、温度、光、溶媒の種類と組成、水の因子が影響することが分かって来た。さらに、C_{60}NW は溶解と再析出を繰り返しつつ成長が進むことが明らかになった。

フラーレンナノファイバーの長さと直径を制御する技術の確立は、軽量でフレキシブルな超伝導線材の作製や安全性の評価をも含む実用化研究にとって重要であり、それらを可能とするフラーレンナノファイバーの成長機構の研究をより一層深めて行くことが必要である。

謝辞

本研究の一部は、平成 24 年度厚生労働科学研究費補助金（化学物質リスク研究事業）「ナノマテリアル曝露による生体毒性の慢性移行及び遅発性に関わる評価手法の開発研究」、及び、平成 24 年度 JST 戦略的国際科学技術協力推進事業「工業用ナノ粒子の健康および環境における潜在的リスク管理に関する研究」の補助を得て行われている。

参考文献

1) Miyazawa K, *J. Nanosci. Nanotechnol.*, **9**, 41-50 (2009).
2) Miyazawa K, Obayashi A and Kuwabara M, *J. Am. Ceram. Soc.*, **84**, 3037-3039(2001).
3) Miyazawa K, Y. Kuwasaki, A. Obayashi and M. Kuwabara, *J. Mater. Res.*, **17**, 83-88(2002).
4) Hoen S, Chopra N G, Xiang X-D, Mostovoy R, Hou J, Vareka W A and Zettl A, *Phys. Rev.* B, **46**, 12737 (1992).
5) Asaka K, Kato R, Miyazawa K and Kizuka T, *Appl. Phys. Lett.*, **89**, 071912 (2006).
6) Nakaya M, Nakayama T, Aono M, *Thin Solid Films*, **464-465**, 327-330 (2004).
7) Rao A M, Zhou P, Wang K A, Hager G T, Holden J M, Wang Y, Lee W-T, Bi X-X, Eklund P C, Cornett D S, Duncan M A, Amster I J, *Science*, **259**, 955-957 (1993).
8) Tachibana M, Kobayashi K, Uchida T, Kojima K, Tanimura M and Miyazawa K, *Chem. Phys. Lett.*, **374**, 279-285 (2003).
9) Watanabe M, Miyazawa K, Kojima K and Tachibana M, *IEEJ Transactions on Sensors and Micromachines*, **128**, 321-324 (2008).
10) Komatsu T, Tachibana M and Kojima K, *Phil. Mag.* A, **81**, 659-666 (2001).
11) US Patent 6890505B2 (2005).
12) Japan Patent 3785454 (2006).
13) Takeya H, Miyazawa K, Kato R, Wakahara T, Ozaki T, Okazaki H, Yamaguchi T and Takano Y, *Molecules*, **17**,4851-4859 (2012).
14) Hebard A F, Rosseinsky M J, Haddon R C, Murphy D W, Glarum S H, Palstra T T M, Ramirez A P, Kortan A R, *Nature*, **350**, 600-601 (1991).
15) Tanigaki K, Ebbesen T W, Saito S, Mizuki J, Tsai J S, Kubo Y and Kuroshima S, *Nature*, **352**, 222 - 223 (1991).
16) Okuda-Shimazaki J, Nudejima S, Takaku S, Kanehira K, Sonezaki S and Taniguchi A, *Health*, **2**, 1463-1466 (2010).
17) Ogawa K, Kato T, Ikegami A, Tsuji H, Aoki A, Ochiai Y and Bird J P, *Appl. Phys. Lett.*, **88** 112109 (2006).
18) Ogawa K, Aoki N, Miyazawa K, Nakamura S, Mashino T, Bird J P and Ochiai Y, *Jpn. J. Appl. Phys.*, **47**, 501-504 (2008).
19) Yang J, Lim H, Choi H C and Shin H S, *Chem. Commun.*, **46**, 2575-2577 (2010).
20) Somani P R, Somani S P and Umeno M, *Appl. Phys. Lett.*, **91**, 173503 (2007).
21) Zhang X, Qu Y, Piao G, Zhao J, Jiao K, *Materials Science and Engineering* B, **175**, 159-163(2010).
22) Minato J, Miyazawa K and Suga T, *Sci. Technol. Adv. Mater.*, **6**, 272-277 (2005).
23) Minato J and Miyazawa K, *Carbon*, **43**, 2837-2841 (2005).
24) Minato J and Miyazawa K, *Diam. Relat. Mater.*, **15**, 1151-1154 (2006).
25) Sathish M, Miyazawa K and Sasaki T, Diam. Relat. Mat., **17**, 571-575 (2008).
26) Sathish M, Miyazawa K and T. Sasaki T, *J.Solid State Electrochem.*, **12**, 835-840 (2008).
27) Sathish M and Miyazawa K, *NANO*, **3**, 409-414 (2008).
28) Ogata H, Motohashi S and Tsuchida S, *J. Phys.: Conf. Ser.*, **159**, 012015 (2009).
29) Miyazawa K, *J. Am. Ceram. Soc.*, **85**, 1297-1299 (2002).
30) Miyazawa K, Minato J, Yoshii T, M. Fujino M and T. Suga, *J.Mater.Res.*, **20**, 688-695 (2005).
31) Miyazawa K, Minato J, Yoshii T and Suga T, *Sci. Technol. Adv. Mater.*, **6**, 388-393(2005).
32) Ringor C L and Miyazawa K, *J. Nanosci. Nanotechnol.*, **9**, 6560-6564 (2009).
33) Zhang X, Jiao K, Piao G, Liu S and Li S, *Synthetic Met.*, **159**, 419-423 (2009).